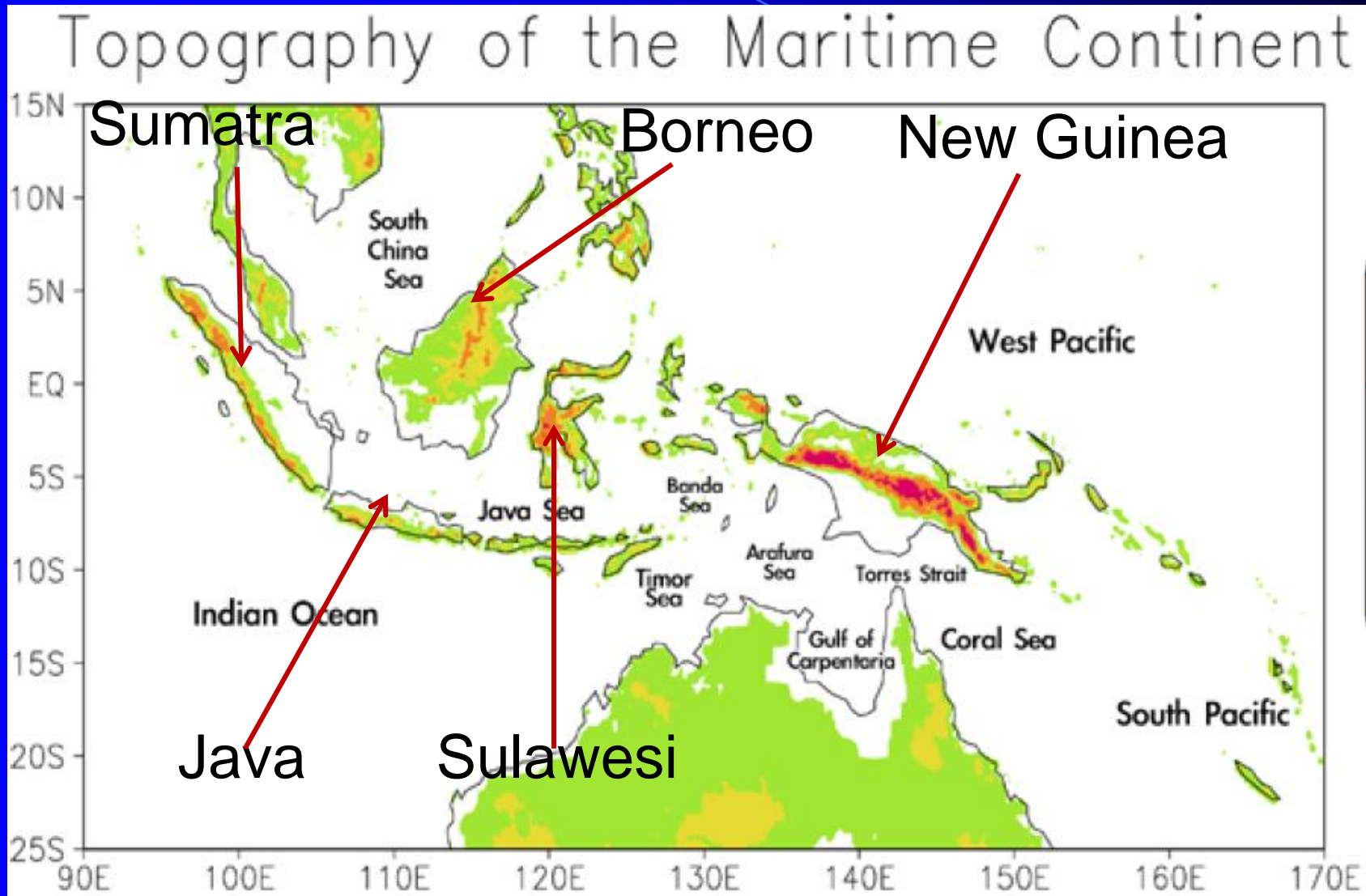


Orographic Effects on the Propagation and Rainfall Modification Associated with the 2007-08 Madden-Julian Oscillation (MJO) Over the New Guinea Mountains

Yuh-Lang Lin, Justin Riley, William Agyakwa
North Carolina A&T State University
Huang-Hsiung Hsu
Academia Sinica

This research is supported by U.S. NSF Award # AGS-1265783

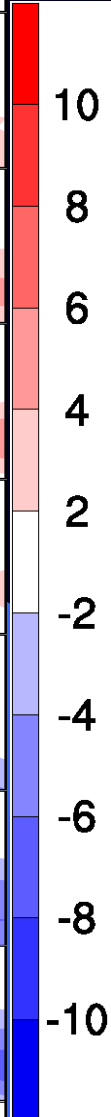
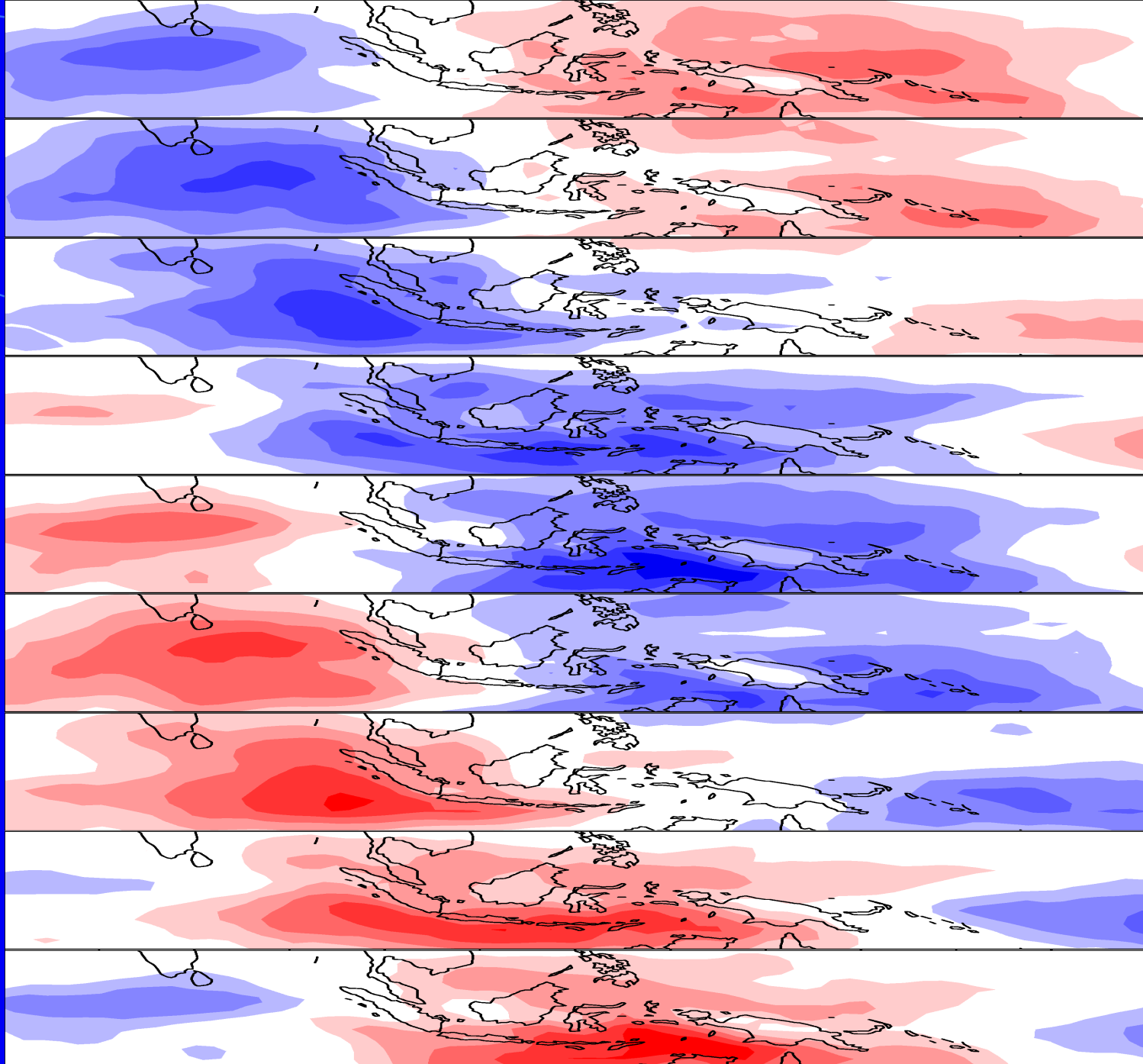
Topography of the Maritime Continent



Hsu and Wu (2009)

OLR (15S-15N)

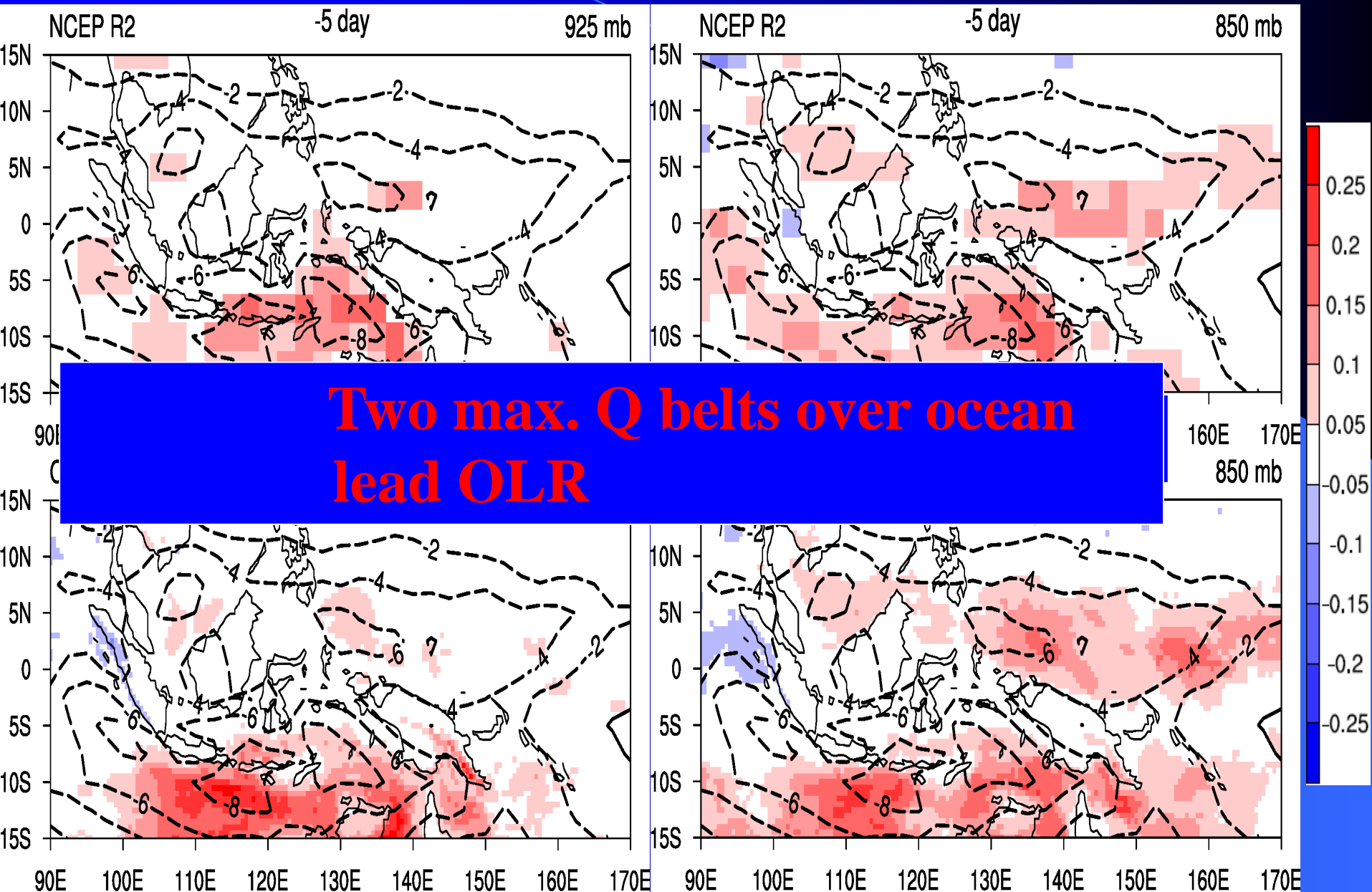
-20
-15
-10
-5
0
5
10
15
20



60E 70E 80E 90E 100E 110E 120E 130E 140E 150E 160E 170E 180

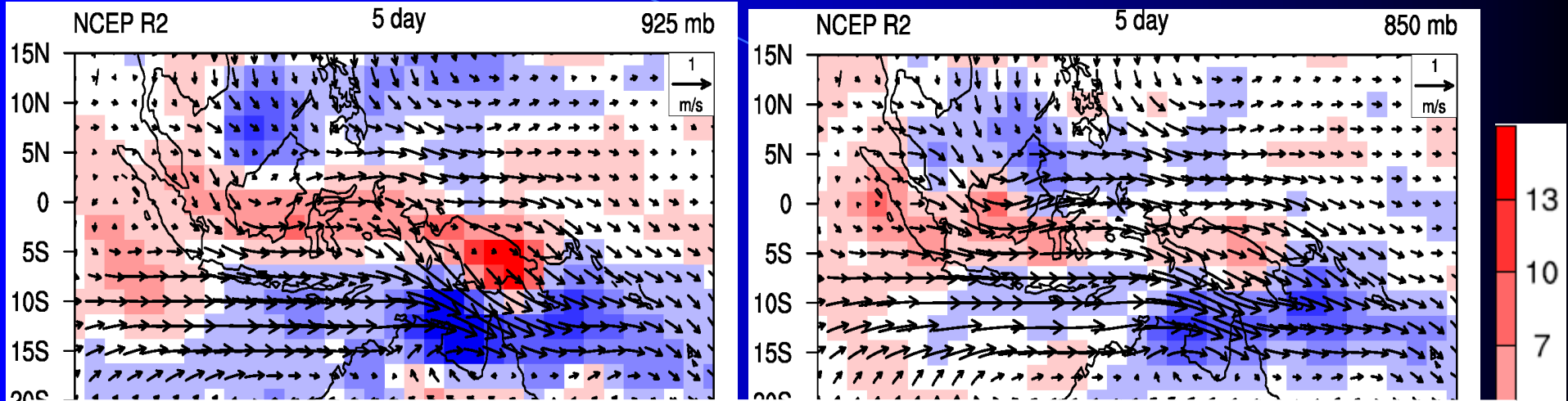
OLR(contour) & Q(shading)

-5 Day

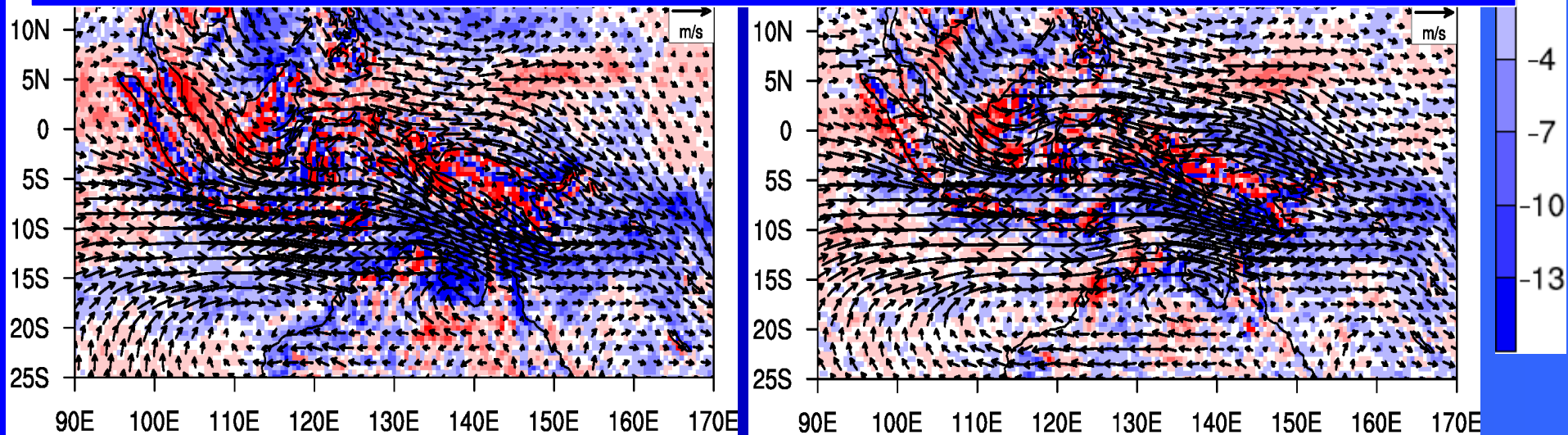


Cir.(contour) & Div-VQ(shading)

5 Day

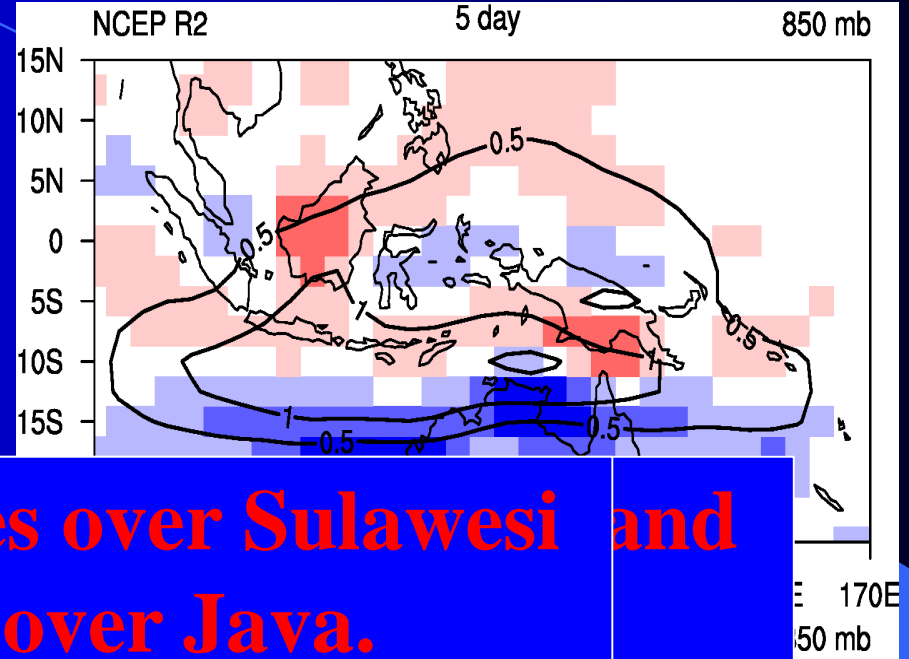
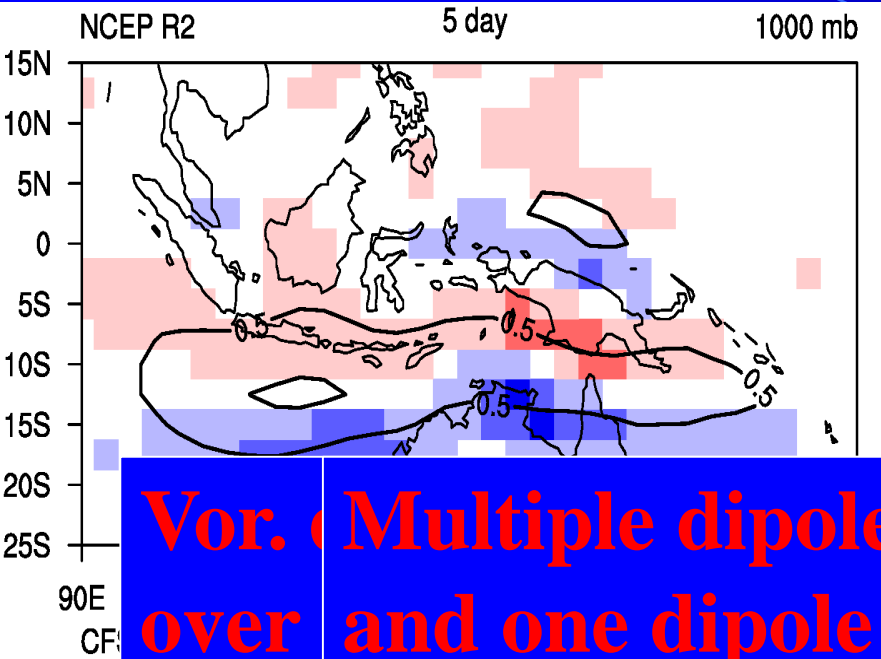


Both flow bifurcation and VQ div.-conv. dipoles appear near Sulawesi and Java.

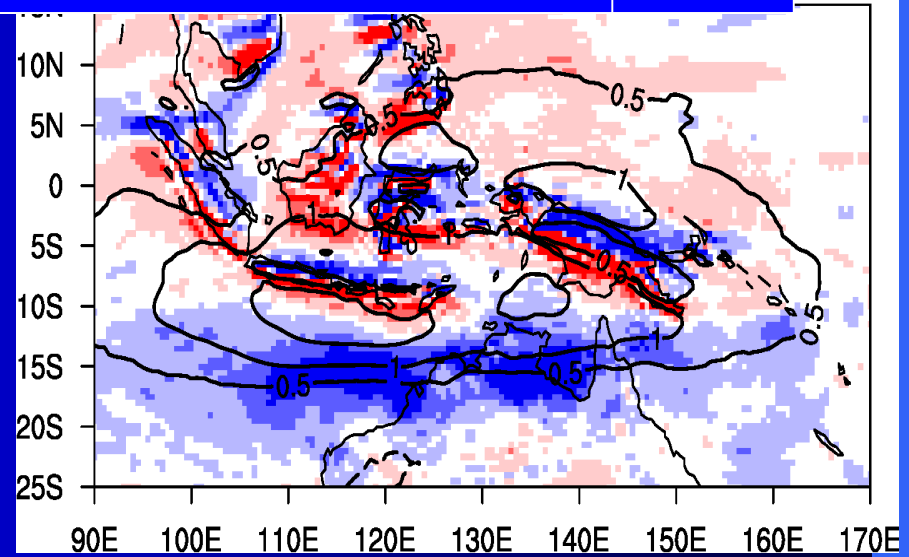
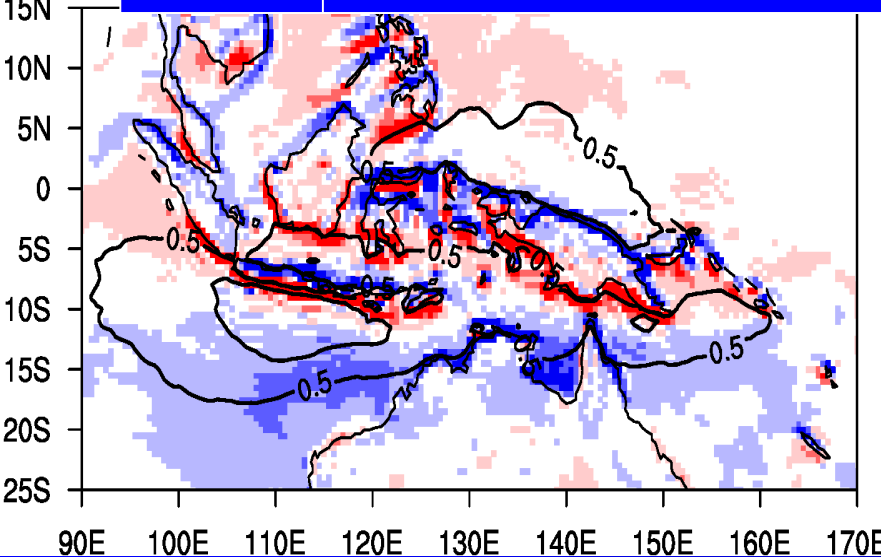


U(contour) & Vor(shading)

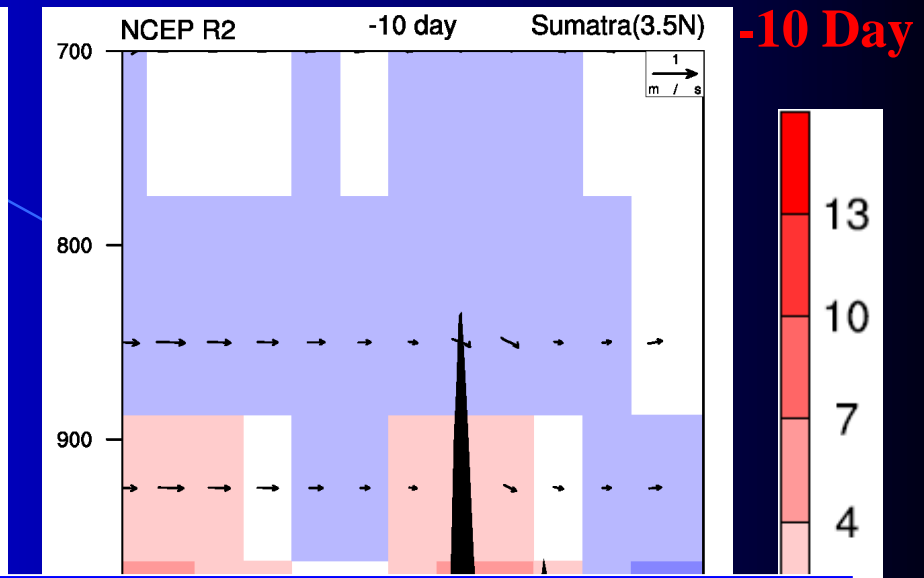
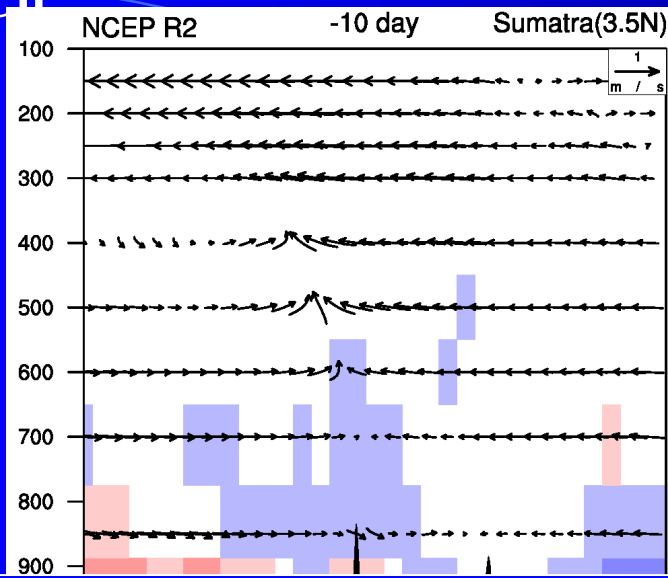
5 Day



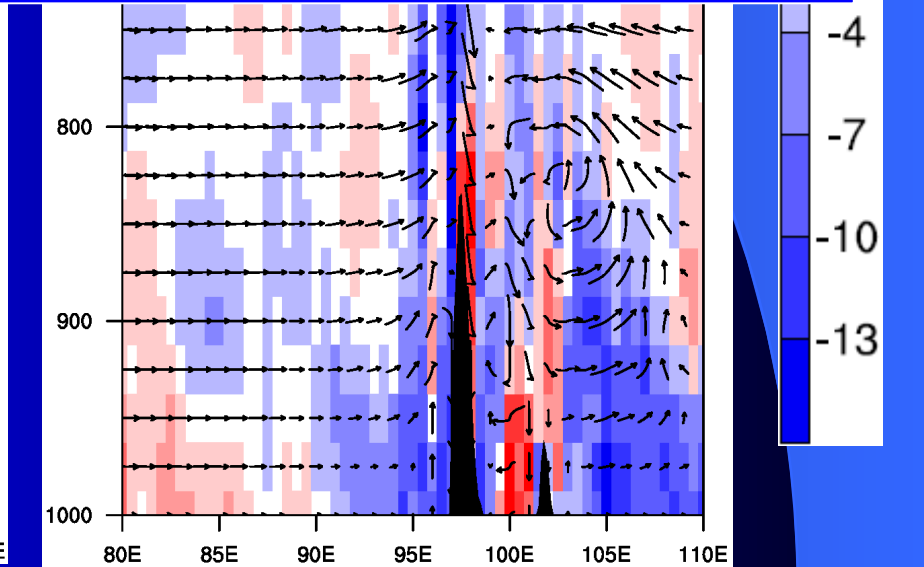
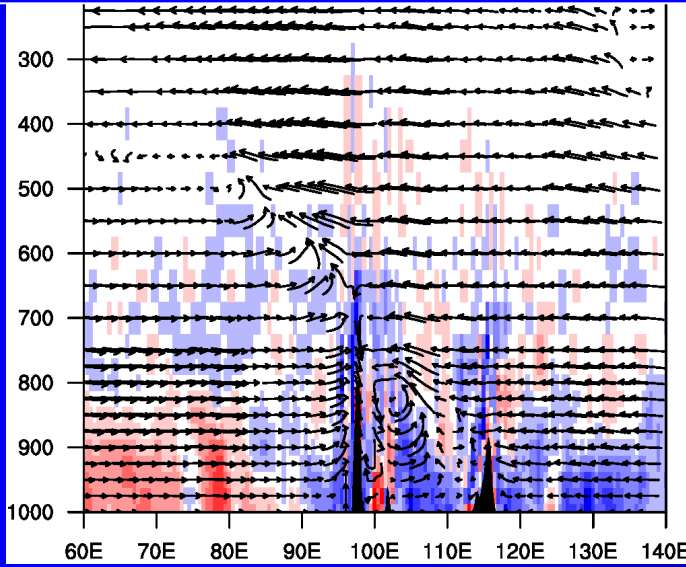
Vor. Multiple dipoles over Sulawesi and over and one dipole over Java.



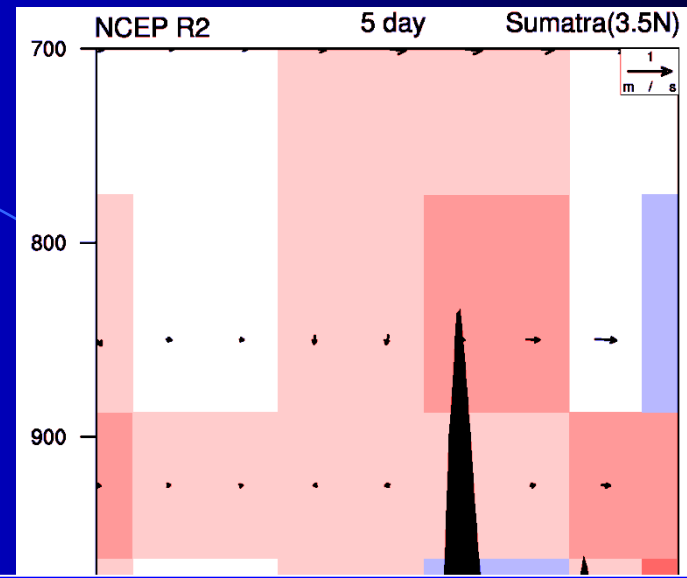
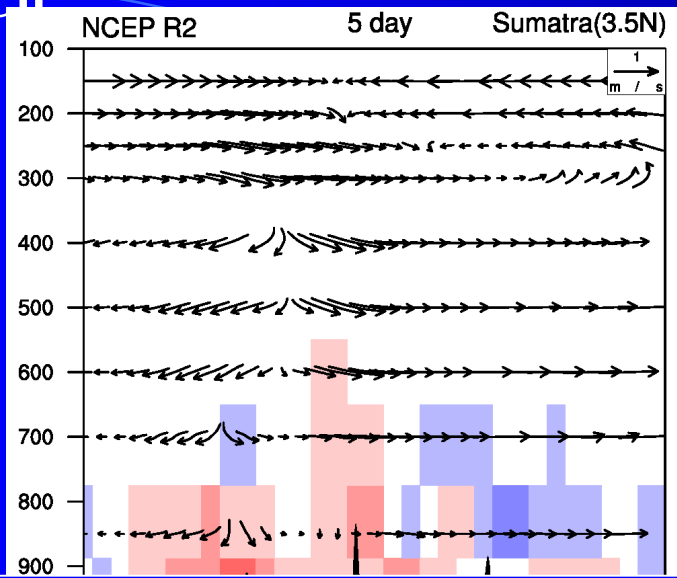
Div-VQ & Cir (3.5N)



**Div-VQ distribution follows local terrain.
Mountain induces anomalous vertical motion.**

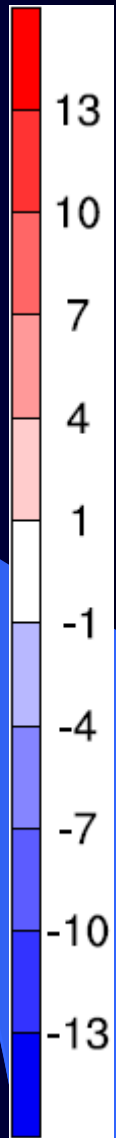
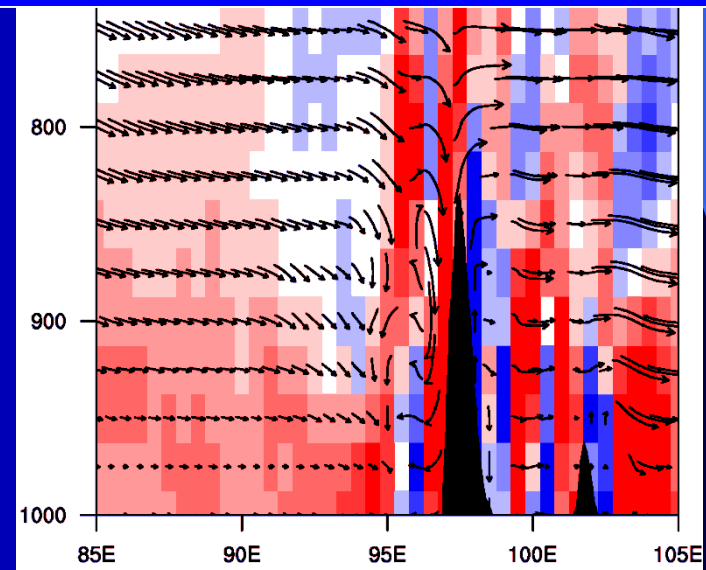
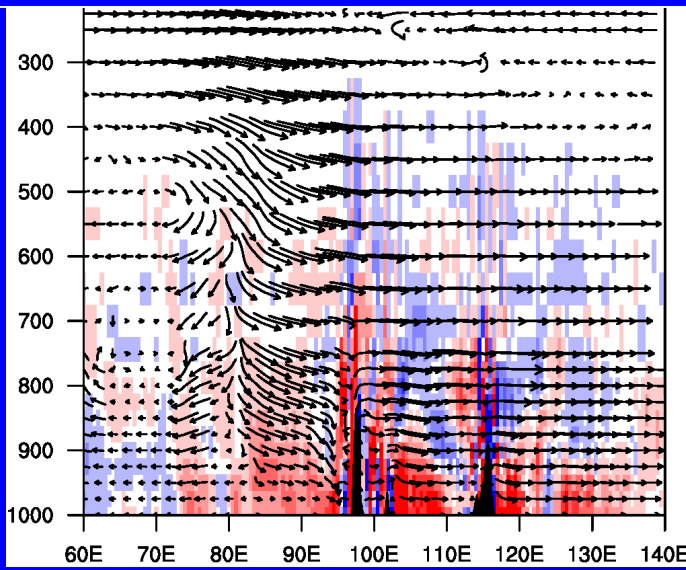


Div-VQ & Cir (3.5N)



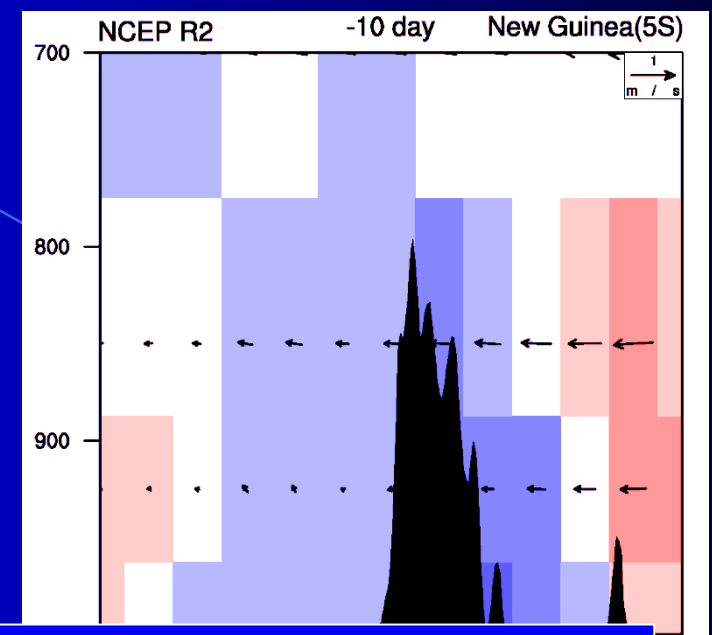
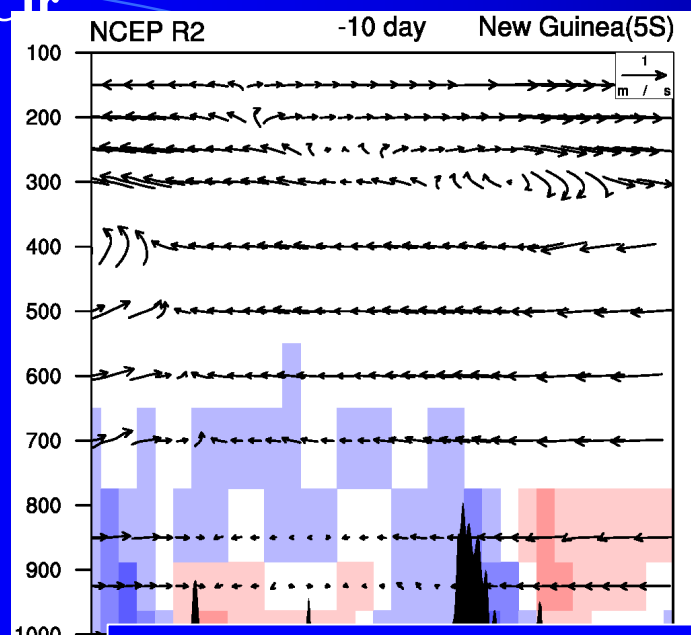
5 Day

Topography causes strong downdraft and westward return flow.



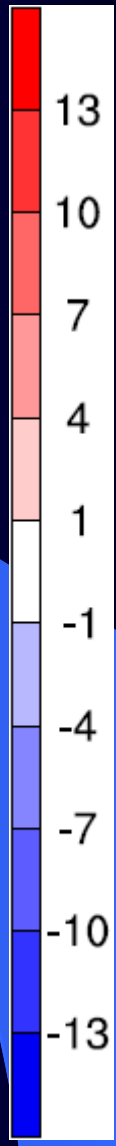
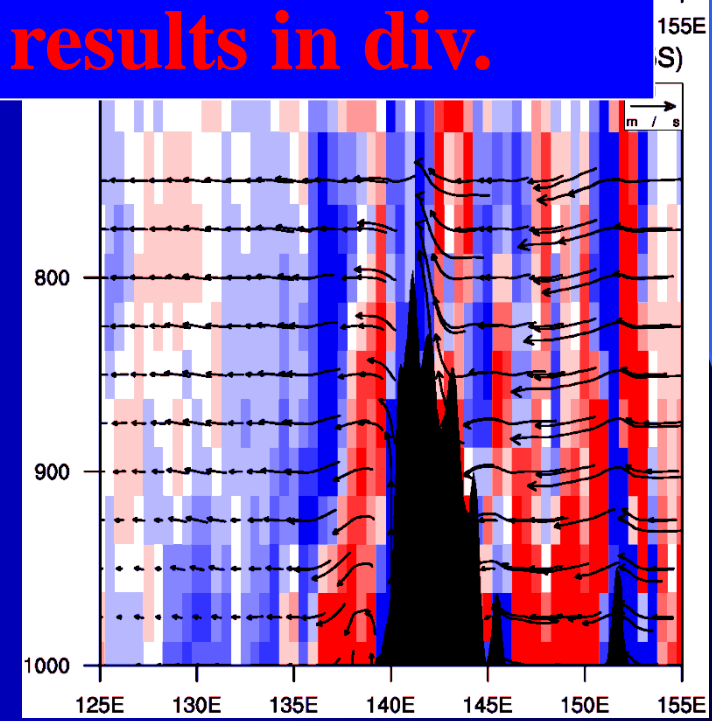
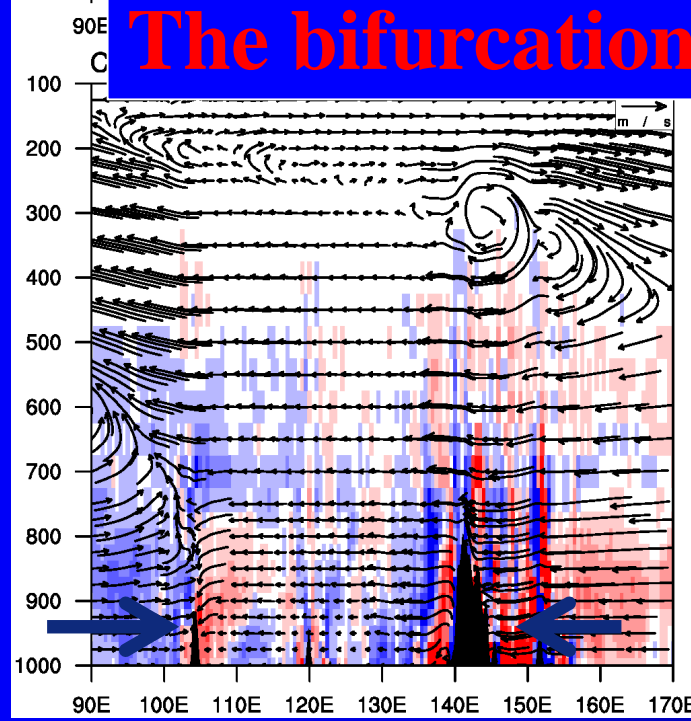
Div-VQ & Cir

(5S)

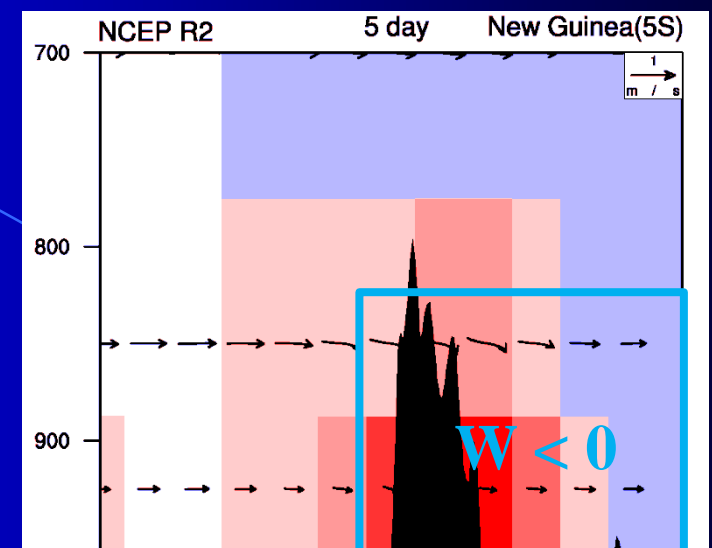
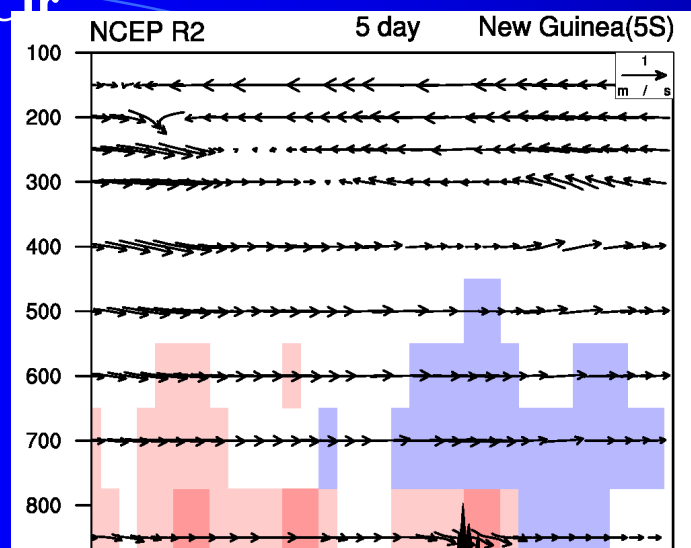


-10 Day

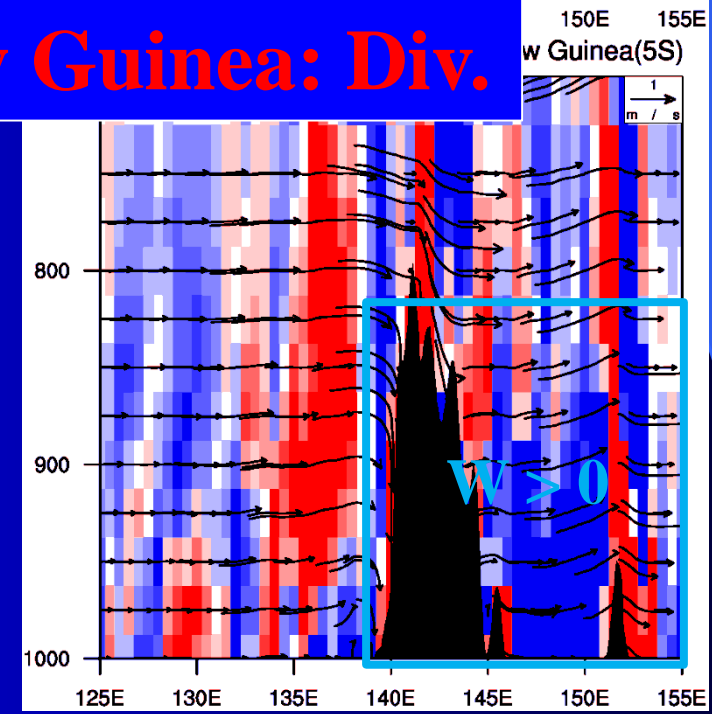
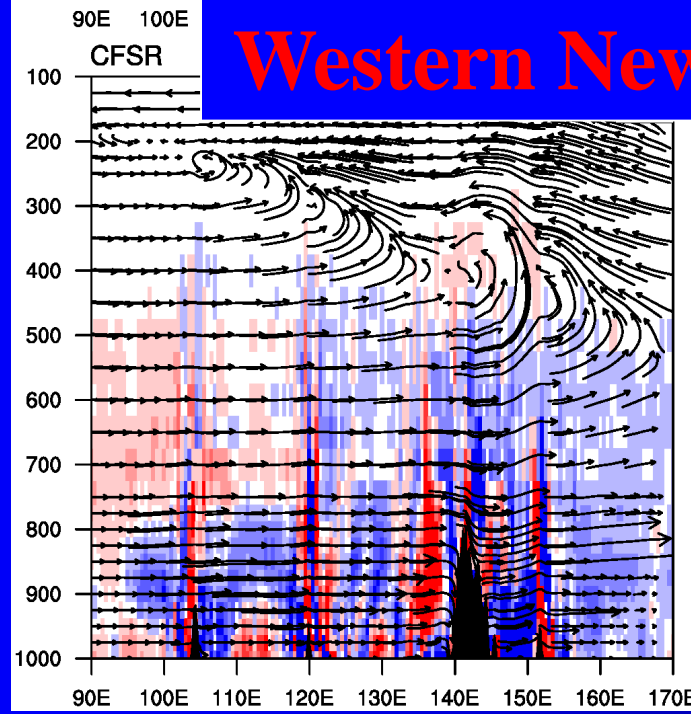
The bifurcation results in div.



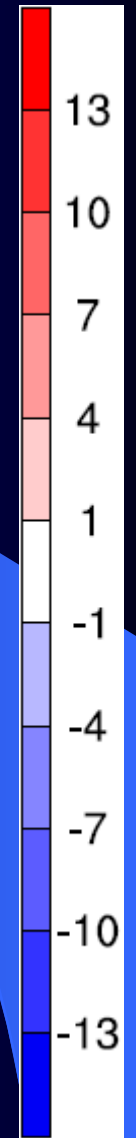
(5S)



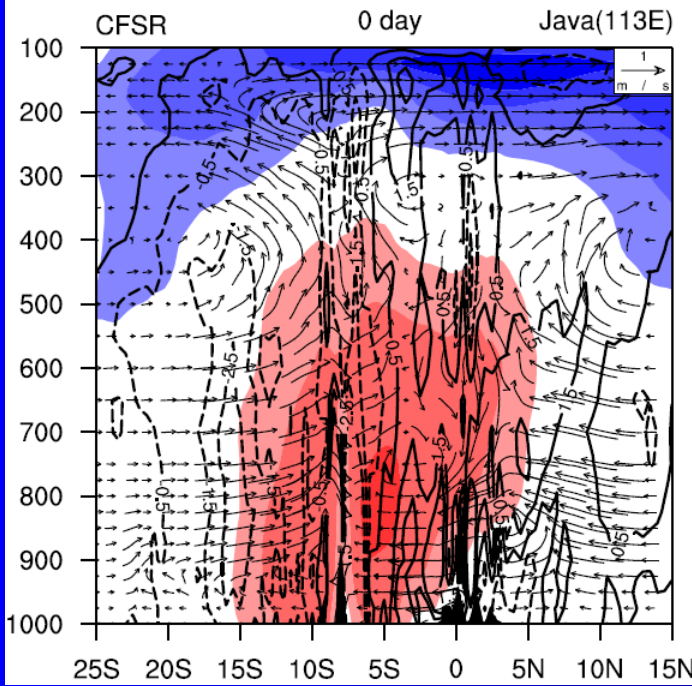
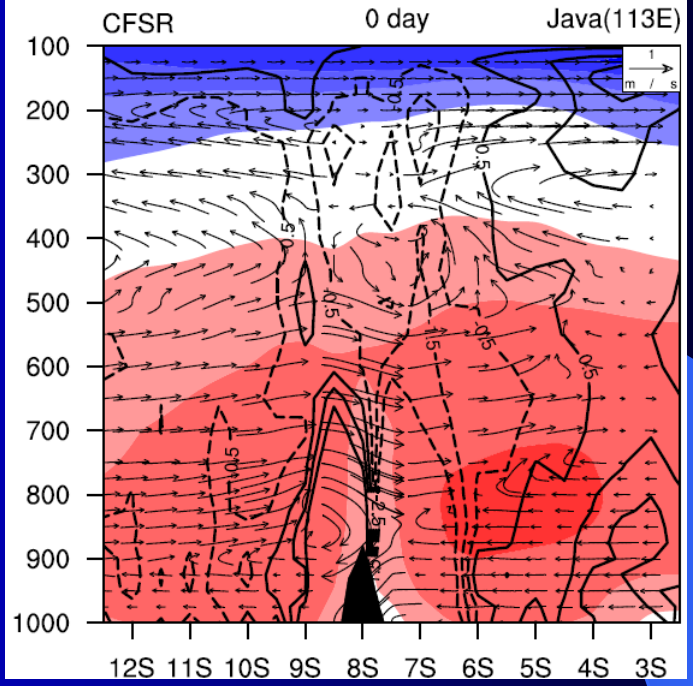
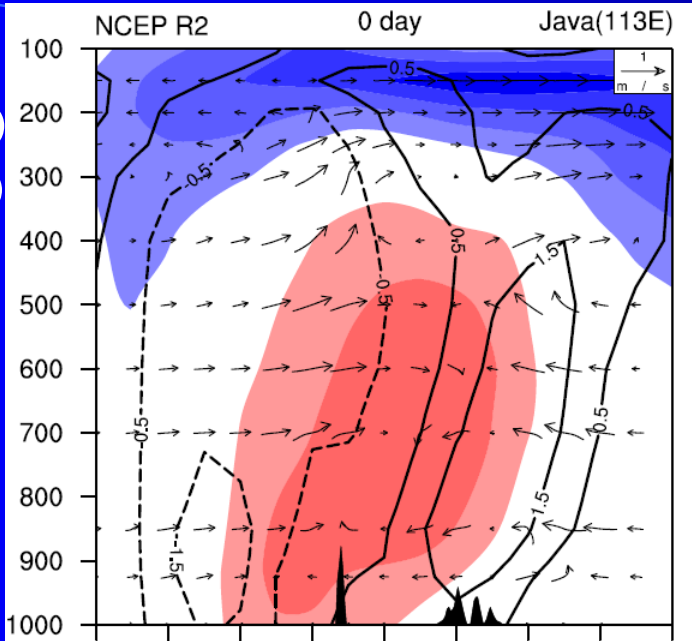
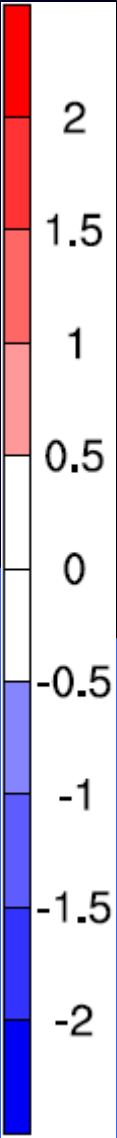
Eastern New Guinea: Con.
Western New Guinea: Div.



5 Day

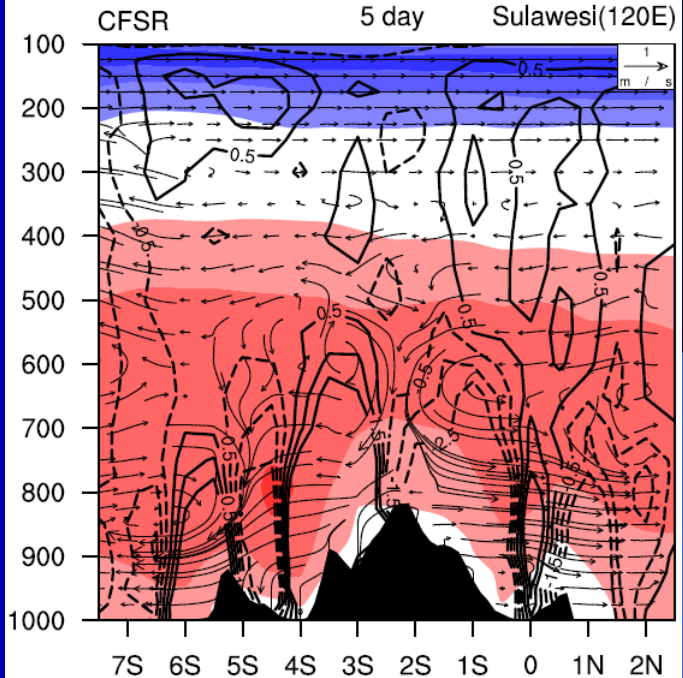
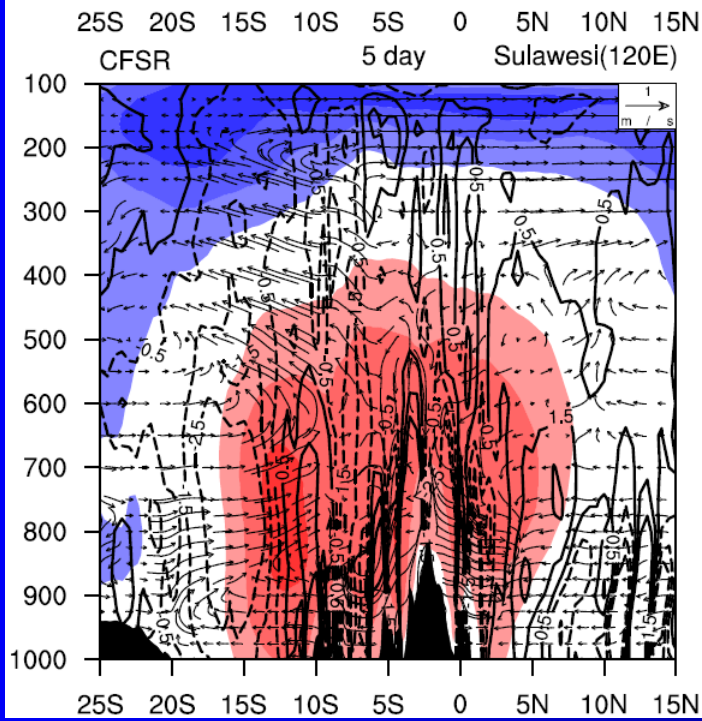
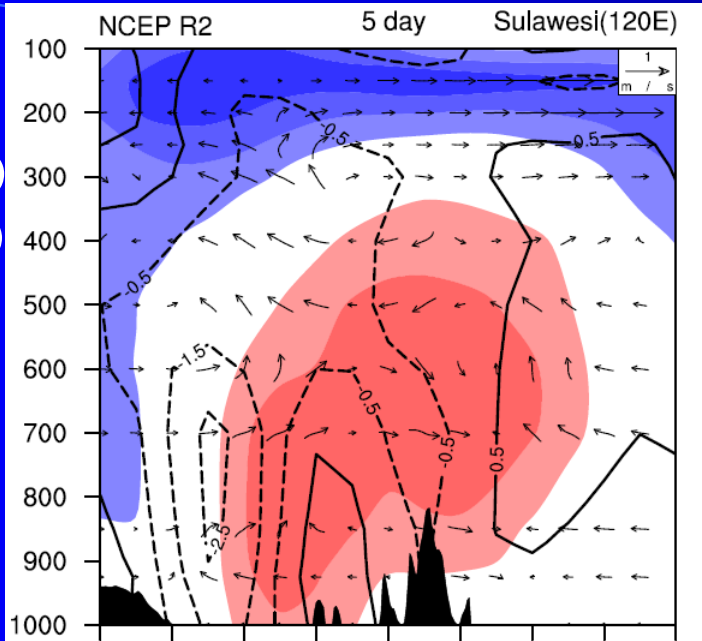
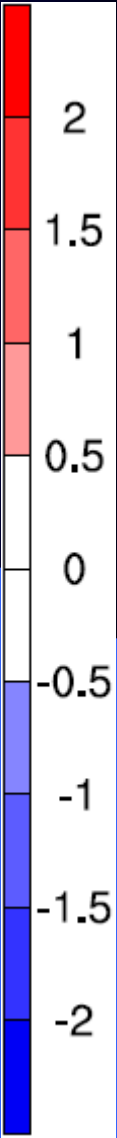


0 Day



Vor.(Contour)
& U(Shading)

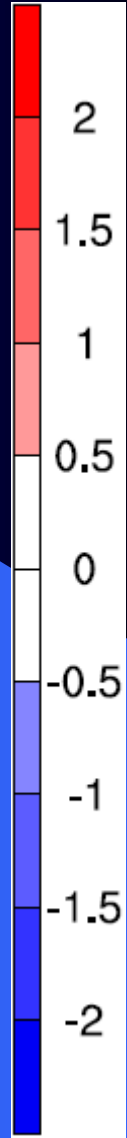
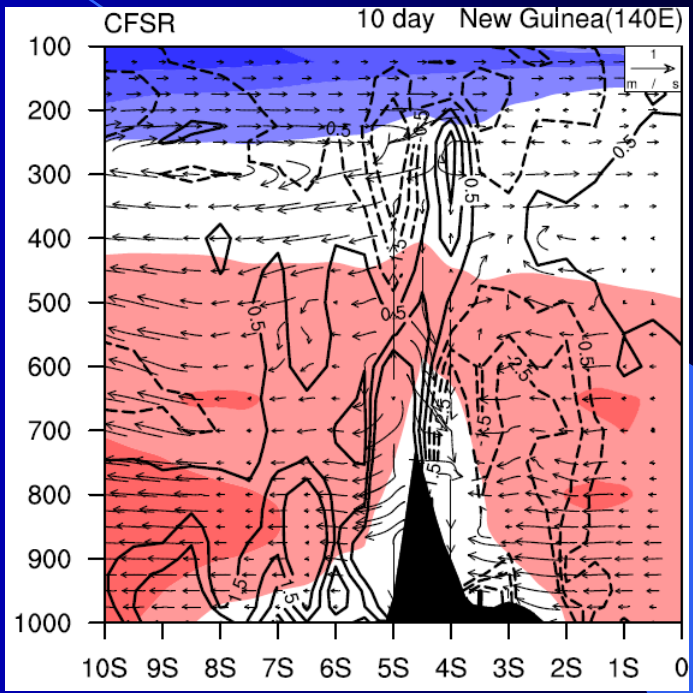
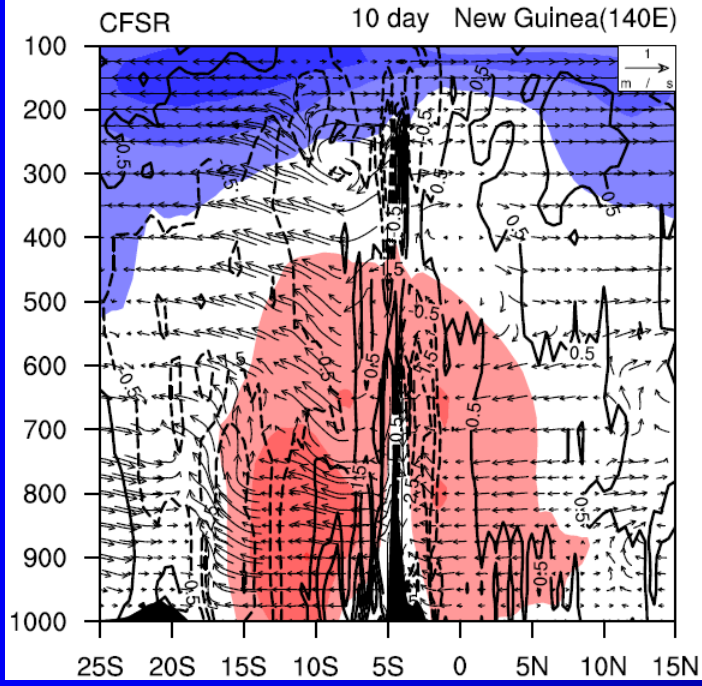
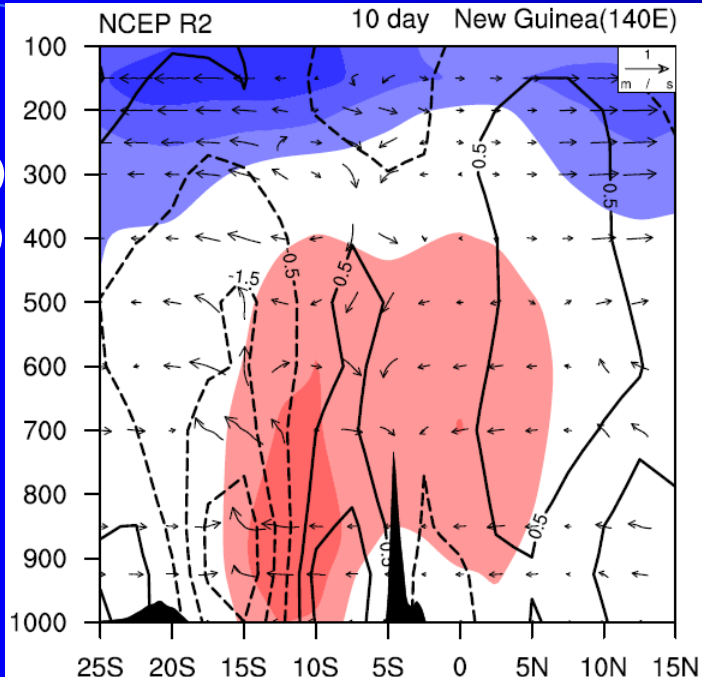
5 Day



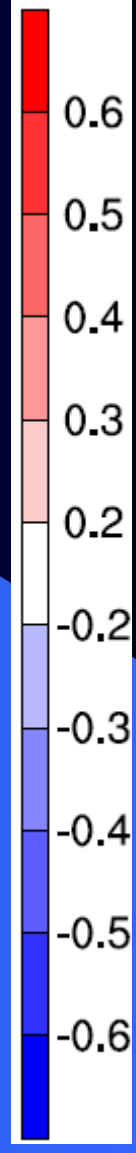
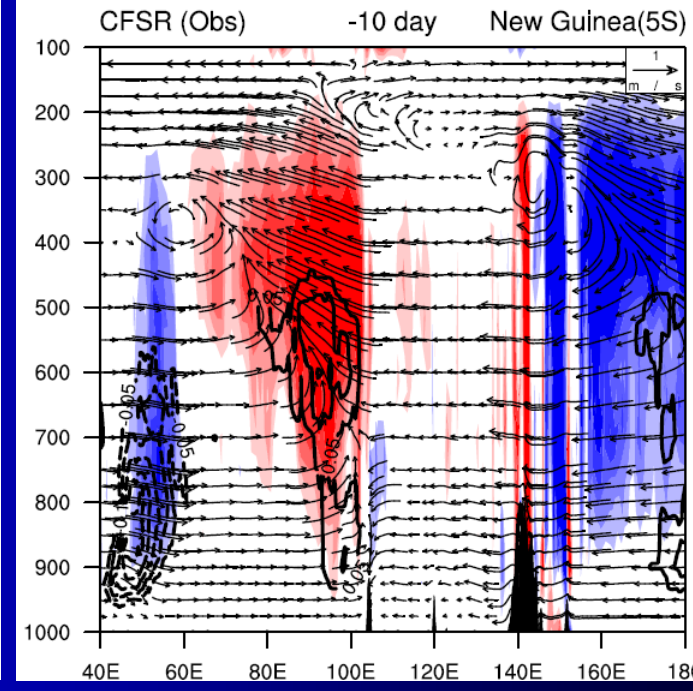
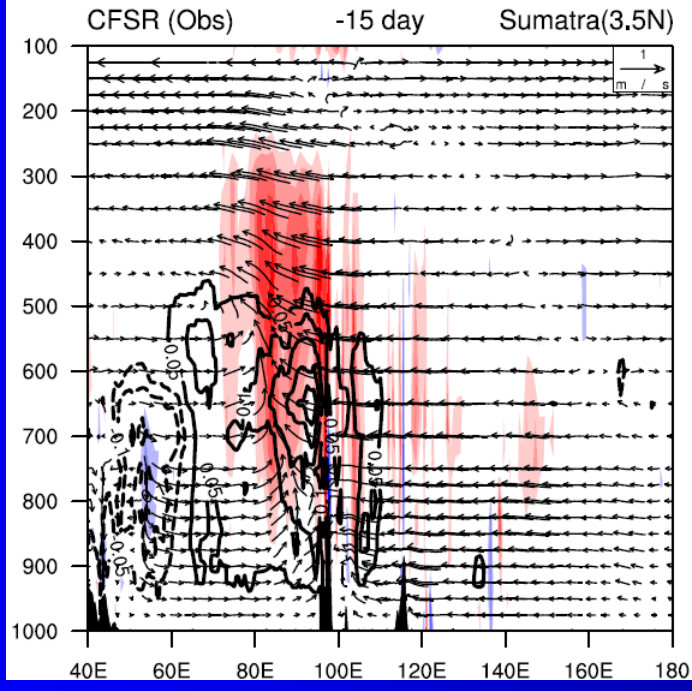
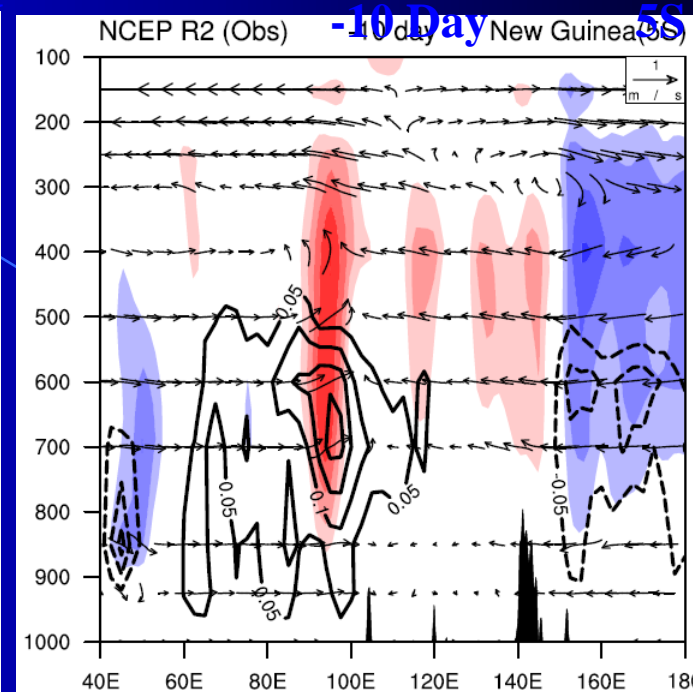
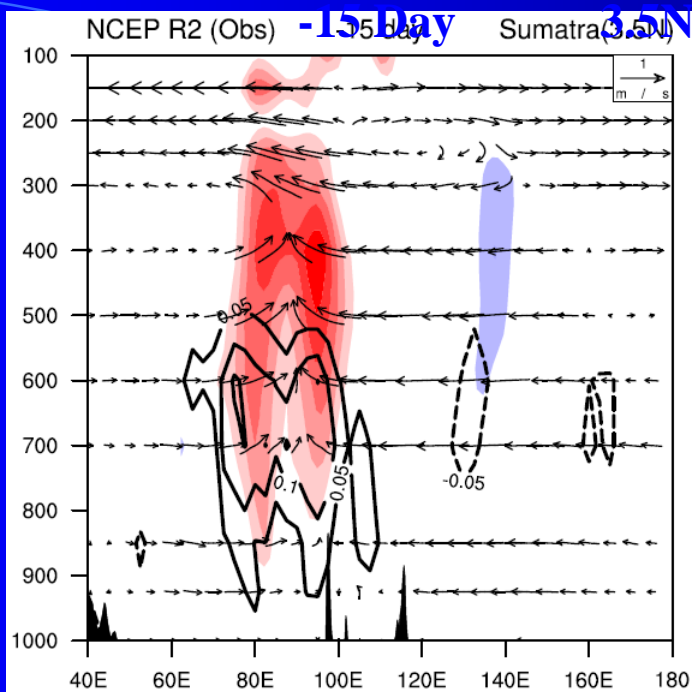
Vor.(Contour)
& U(Shading)

10 Day

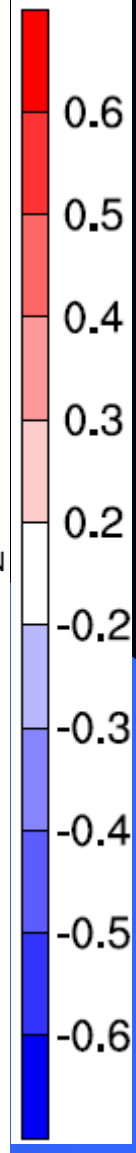
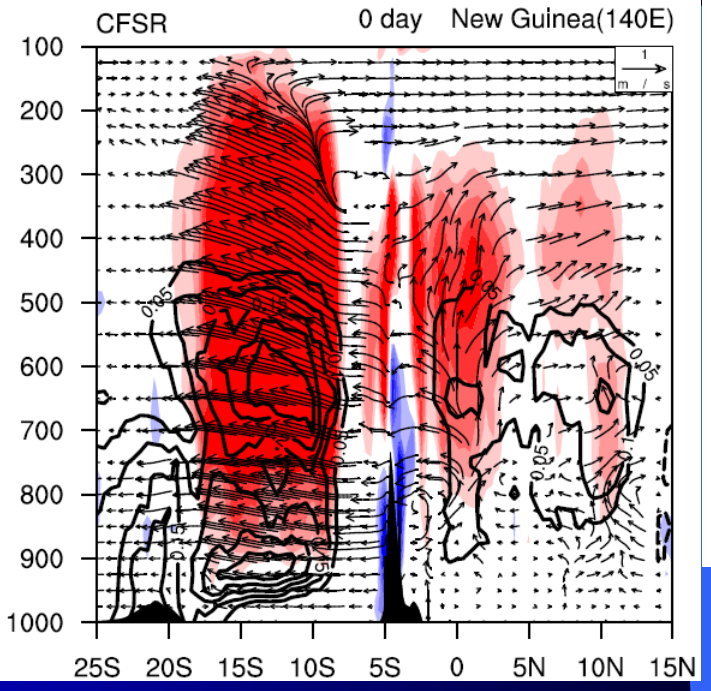
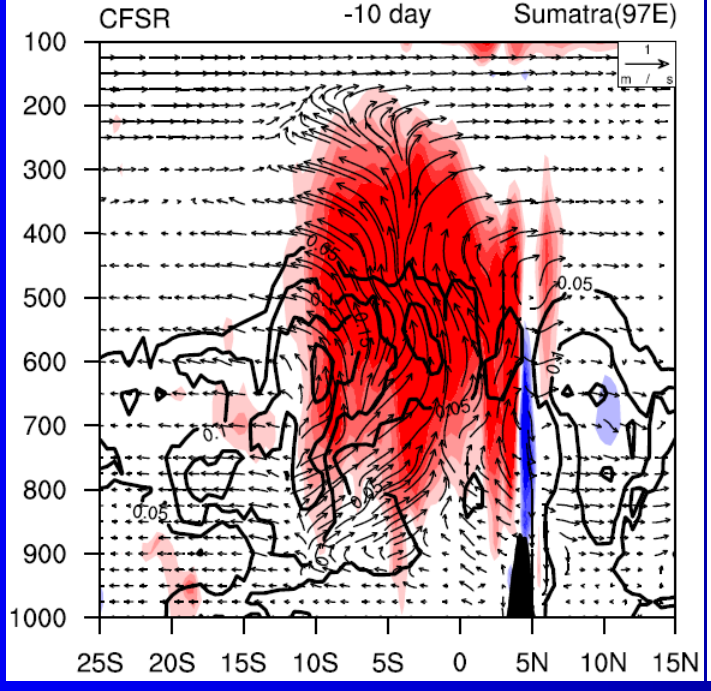
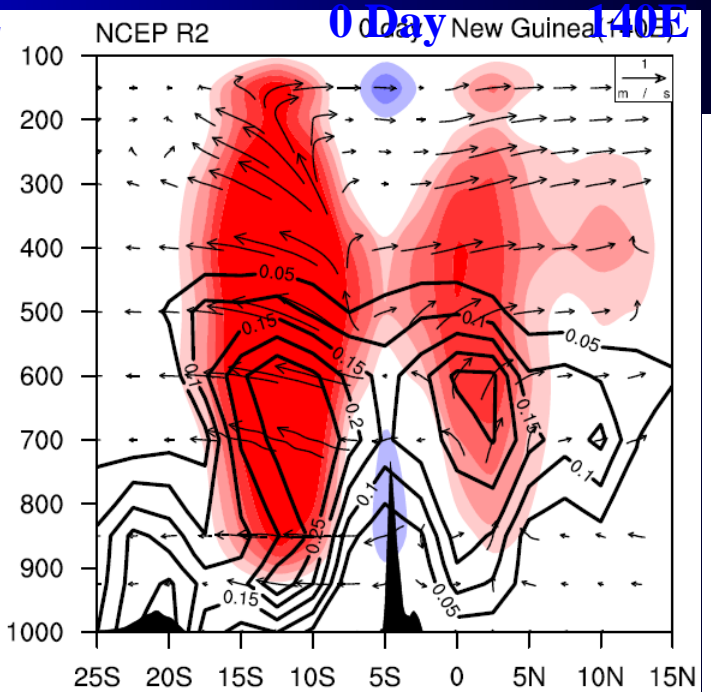
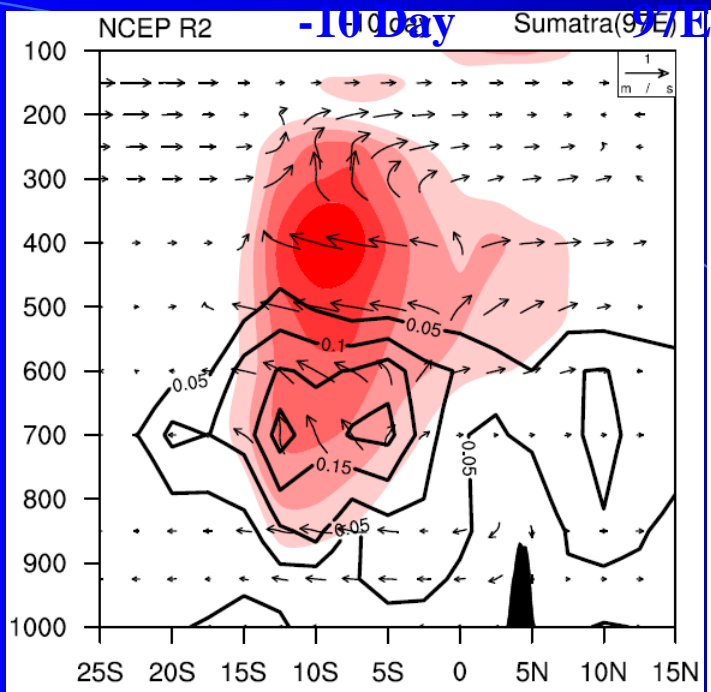
Vor.(Contour)
& U(Shading)



Q1(Shading) & Q(Contour)

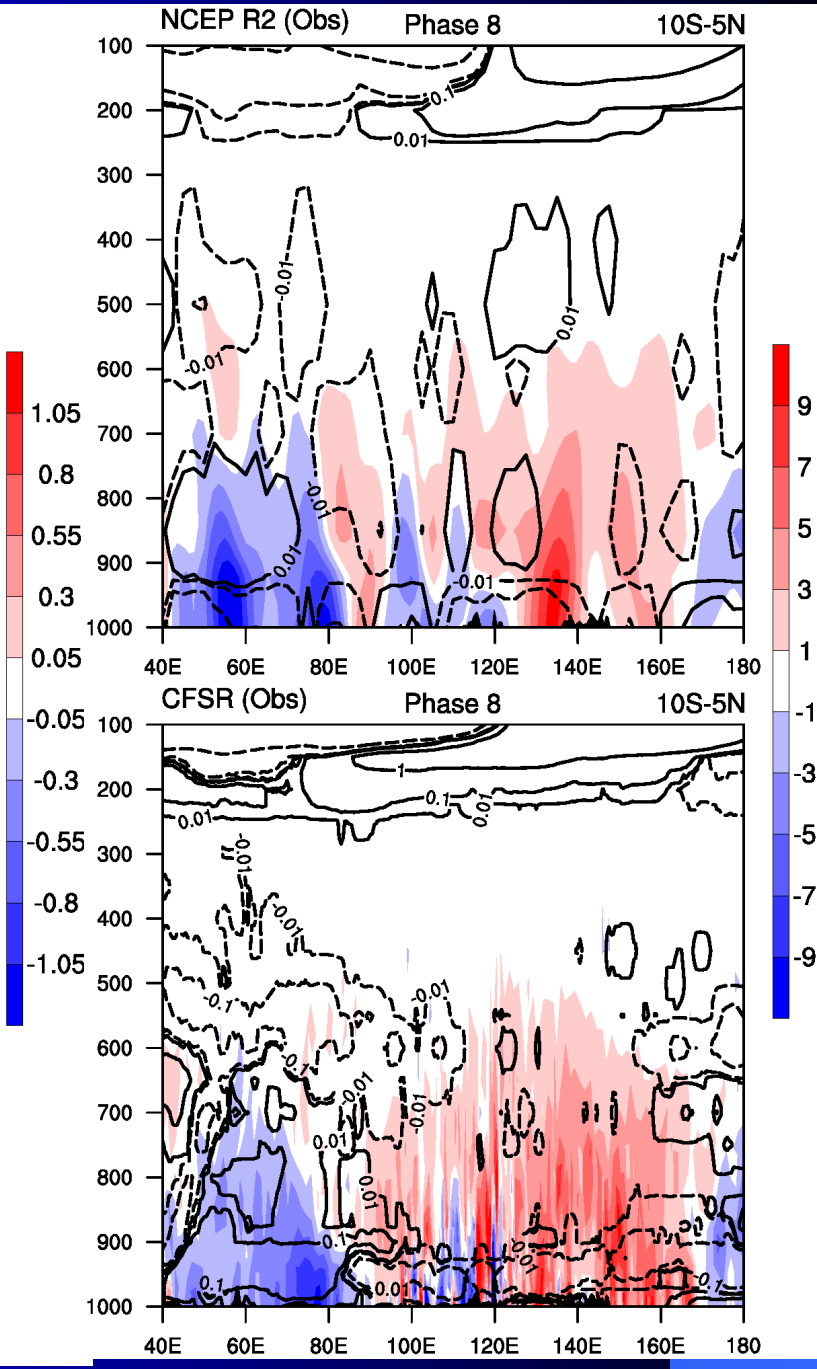
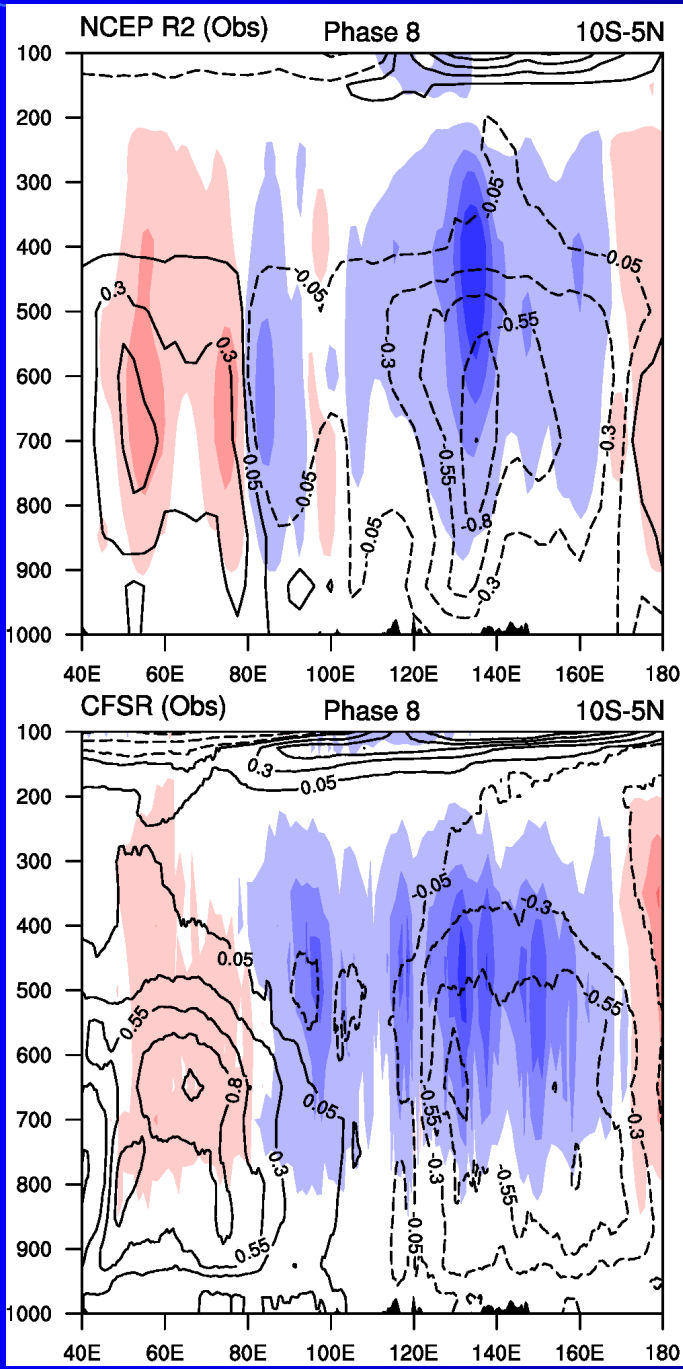


Q1(Shading) & Q(Contour)



Left :
Q1(Shading)
 θ_e (Contour)

Right :
Div-VQ(Shading)
MSS(Contour)



Part A: Orographic Influences on TC-Rain

A.1 Introduction

World Records of Extreme Precipitation

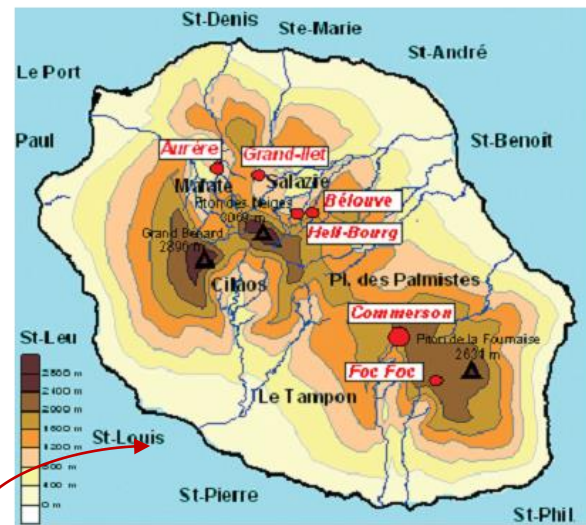
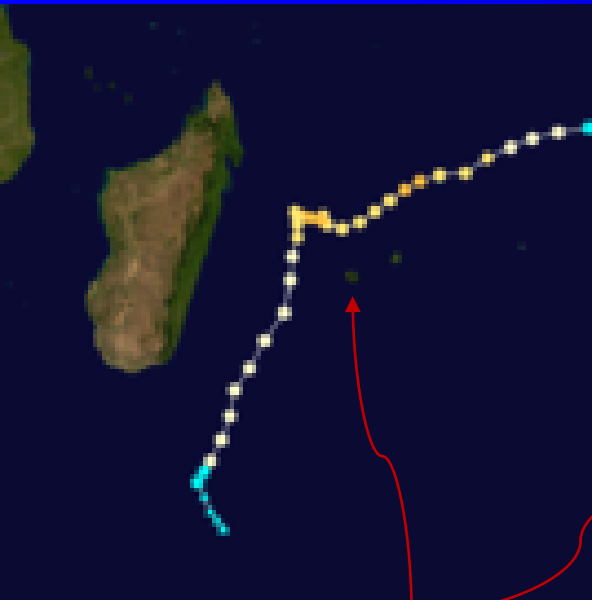
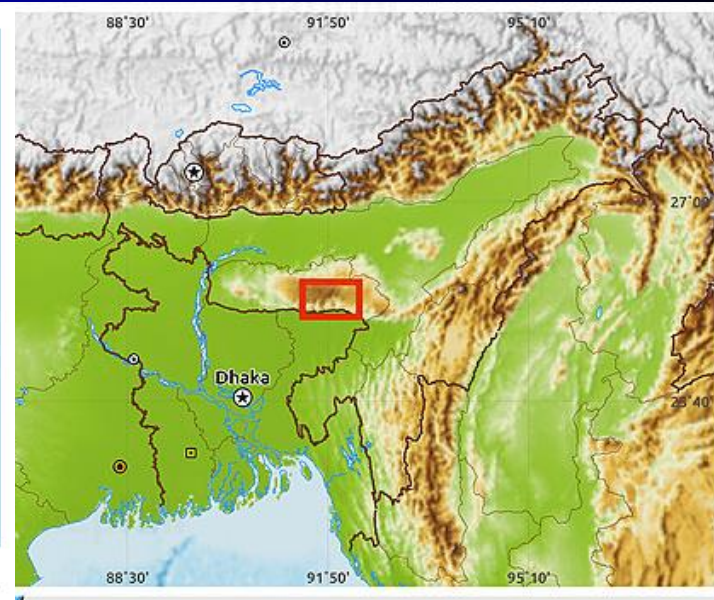


FIG. 2. Topographic map of La Réunion Island.



La Réunion, France

Cherrapunji, India

12 h: 1,144 mm; Cilaos, Réunion, 1/8/1966, with TC Denise.

24 h: **1,825 mm**; Cilaos, Réunion, 1/7–8/1966, with TC Denise. [↔ **1,403 mm, Alisan, Morako (2009)**; **1,092 mm, Alvin, Texas, TS Claudette (1979)**]

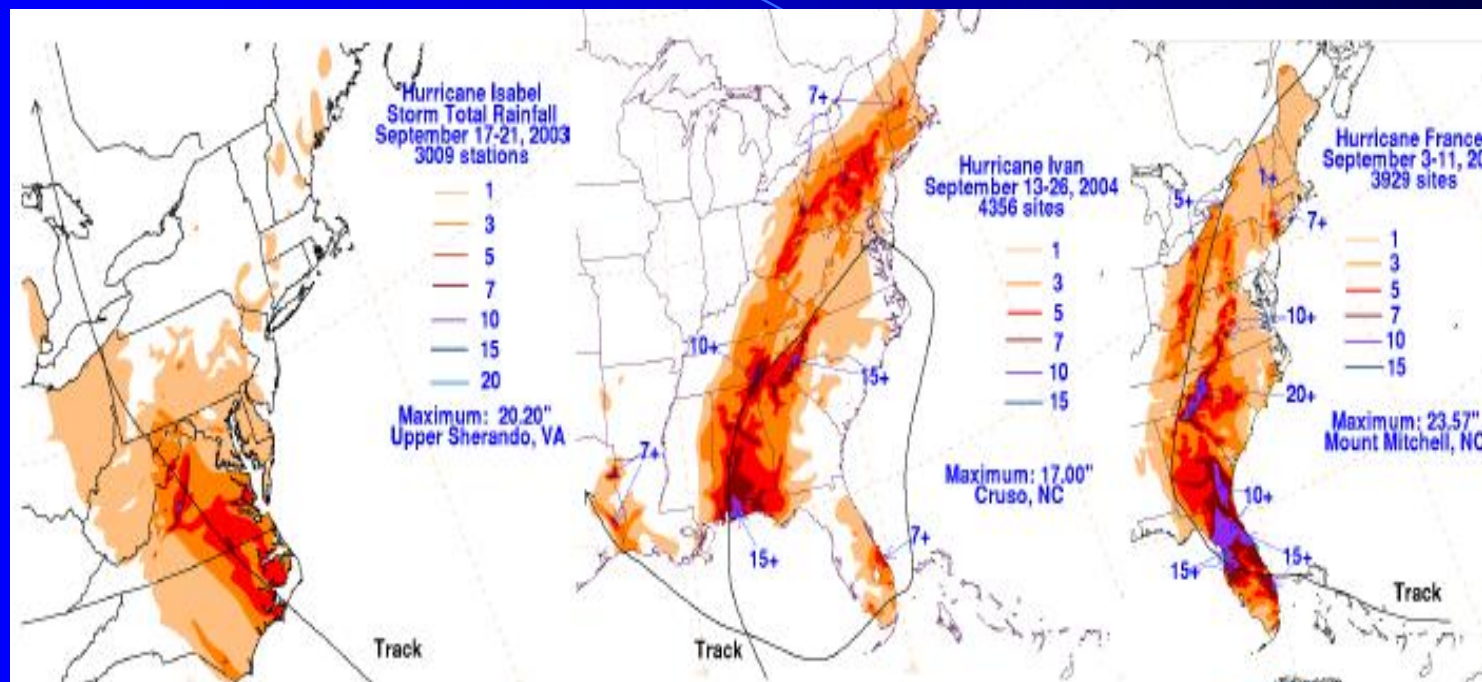
48 h: 2,493 mm; Cherrapunji, Meghalaya, India, 6/15–16/1995, monsoon current, steep mountain

72 h: 3,929 mm; Commerson, Réunion, 2/24–26/2007, oro rain with TC Gamede.

96 h: 4,869 mm; Commerson, Réunion, 2/24–27/2007, oro rain with TC Gamede.

Q: Why Reunion? What are the common ingredients for heavy oro-TC rain?

Example 1: Rainfall Enhancement for hurricanes passing over Appalachian Mountains in the U.S.



Isabel (2003) Type A
max rainfall over
mountains of central
Virginia

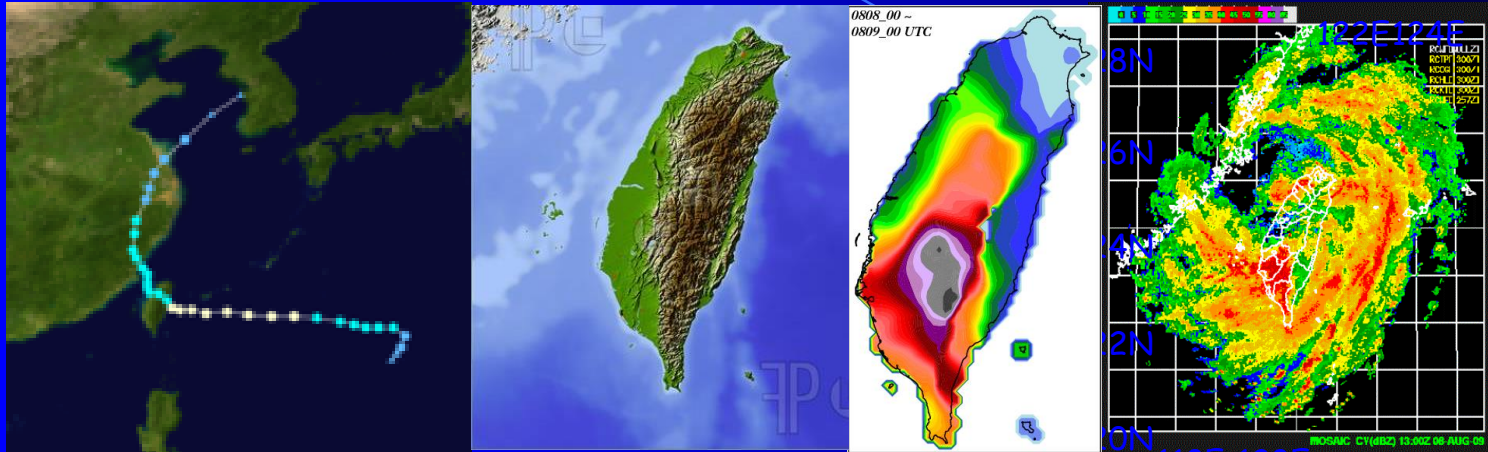
Ivan (2004) Type B
heavy rainfall is located
along eastern slopes of
Appalachians

Frances (2004) Type C
heaviest rainfall falling on
eastern slopes of western
NC

Distribution of orographic TC-Rain is strongly affected by TC tracks!

Example 2: Effects of Taiwan's Central Mountain Range (CMR) on Typhoons

Q1: What caused extremely heavy rainfall?



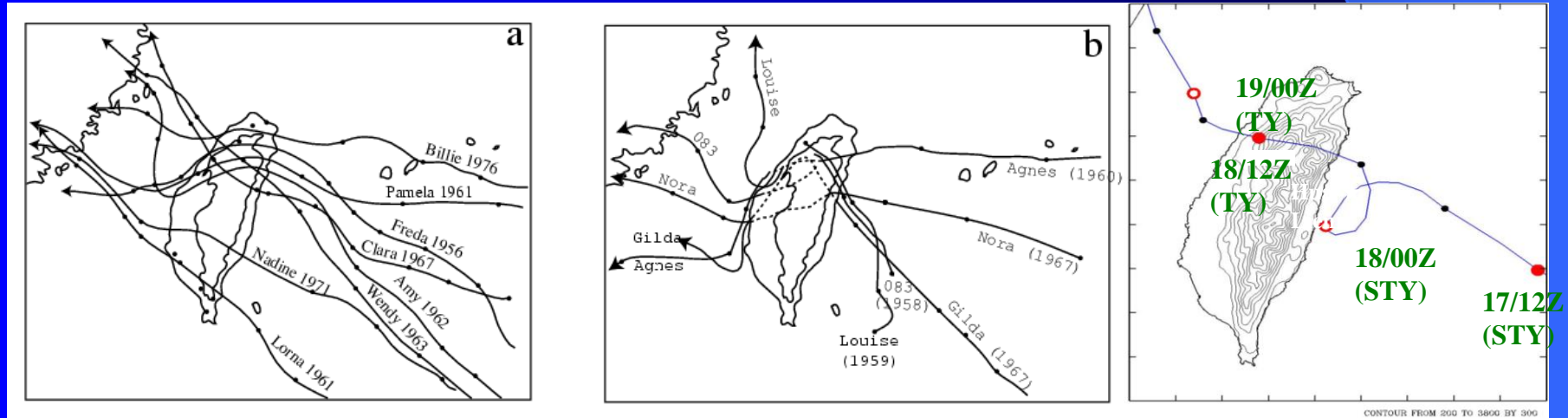
Typhoon Morakot (2009)

CMR

8/8-8/9 rain

8/9/13UTC radar

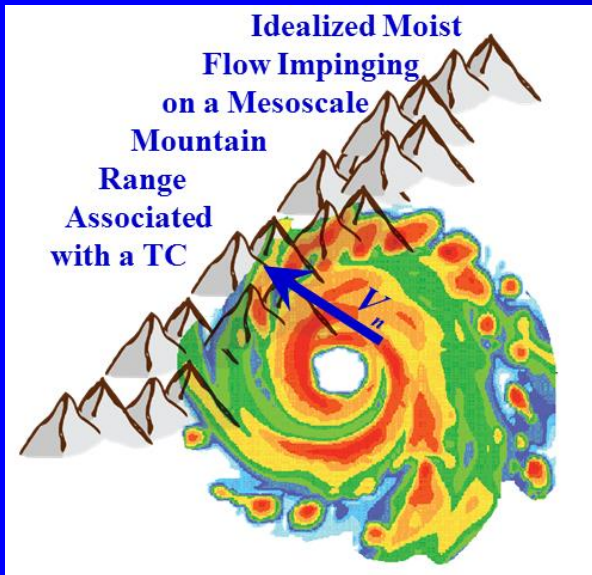
Q2: What caused track continuity, discontinuity and looping?



S.-T. Wang (1980), Chang (1982), (Lin 2007)

Jian and Wu (2006)

For orographic TC-rain, we are particularly interested in addressing the following questions:



- What are the key ingredients?
- How does the mountain interact with or initiate convection in producing heavy rainfall under high wind condition?

For orographic influences on TC track, we are particularly interested in finding the **key mechanisms** for track deflection and their relevant **control parameters**.

A.2 Moist Flow Regimes

For nondimensional control parameters, we consider the following key dimensional control parameters for moist flow over mountains: U, N, h, a

There exist 3 nondimensional control parameters:

$$U/Nh, Ua/N, h/a$$

Based on Buckingham- Π theorem, there are only 2 independent, nondimensional parameters ($4 - 2 = 2$).

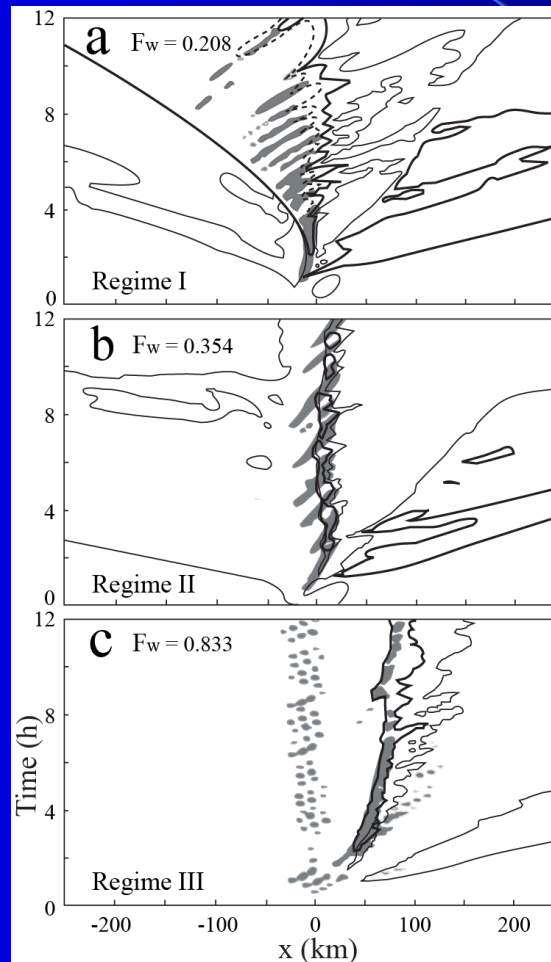
Thus, for example, we may choose (1) $U/N_m h$ or $U/N_m h$ (nonlinearity) and (2) h/a (steepness).

Regimes for a conditionally unstable flow over mesoscale mountain

Small F
(small U
with N & h fixed)

Moderate F
(moderate U)

Large F
(large U)



Convective cells
move downstream,
but precip system
moves upstream

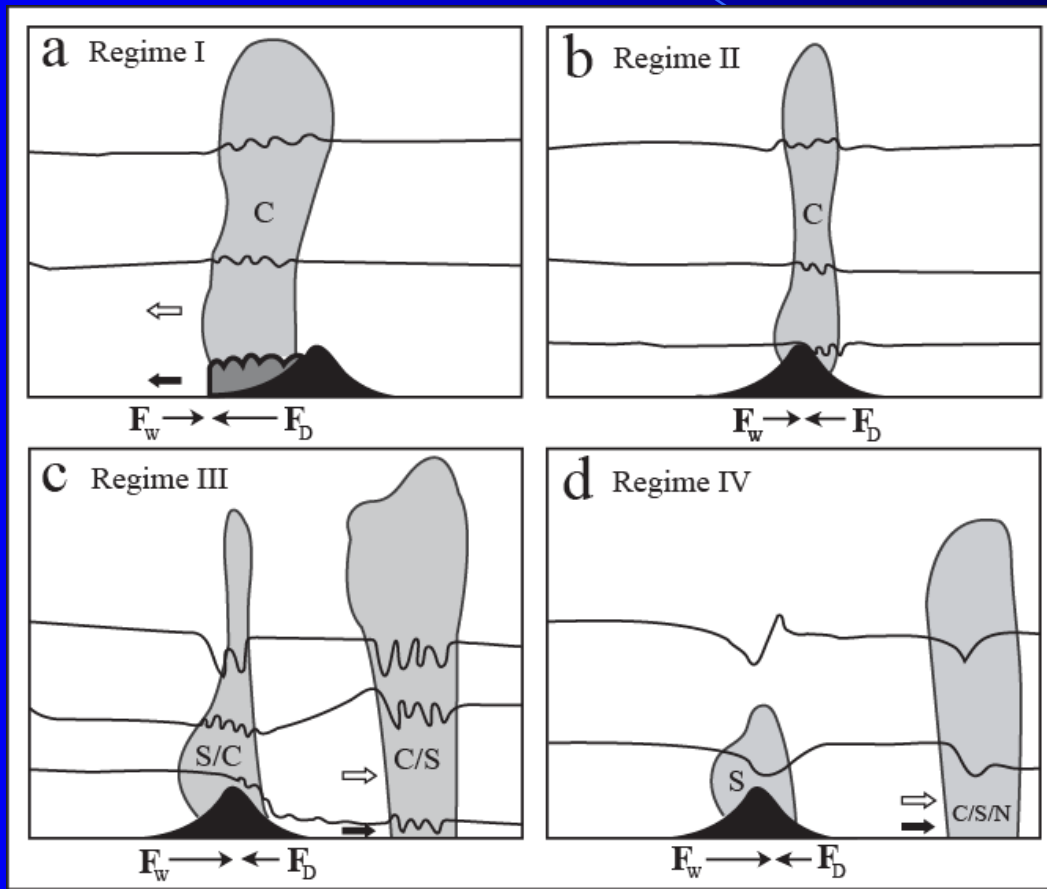
Precip system stays
stationary

Precip system moves
downstream

(Chu & Lin 2000 JAS)

With CAPE added, 4 flow regimes can be identified

Small F_w
Large CAPE



Small F_w
Small CAPE

Large F_w
Large CAPE

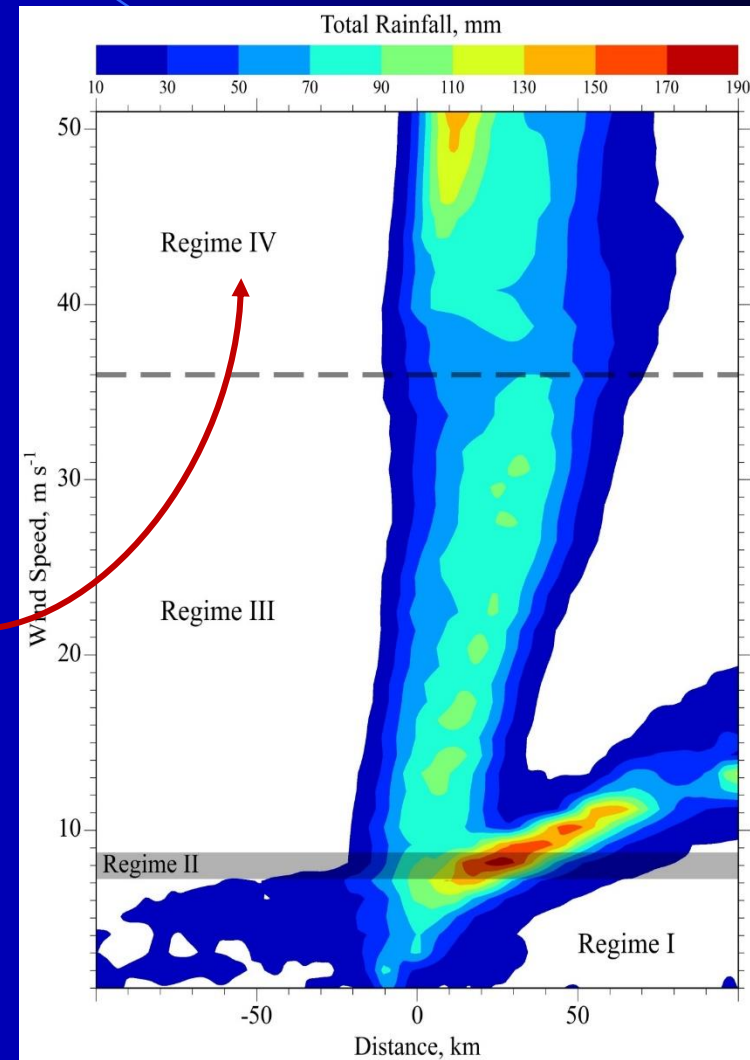
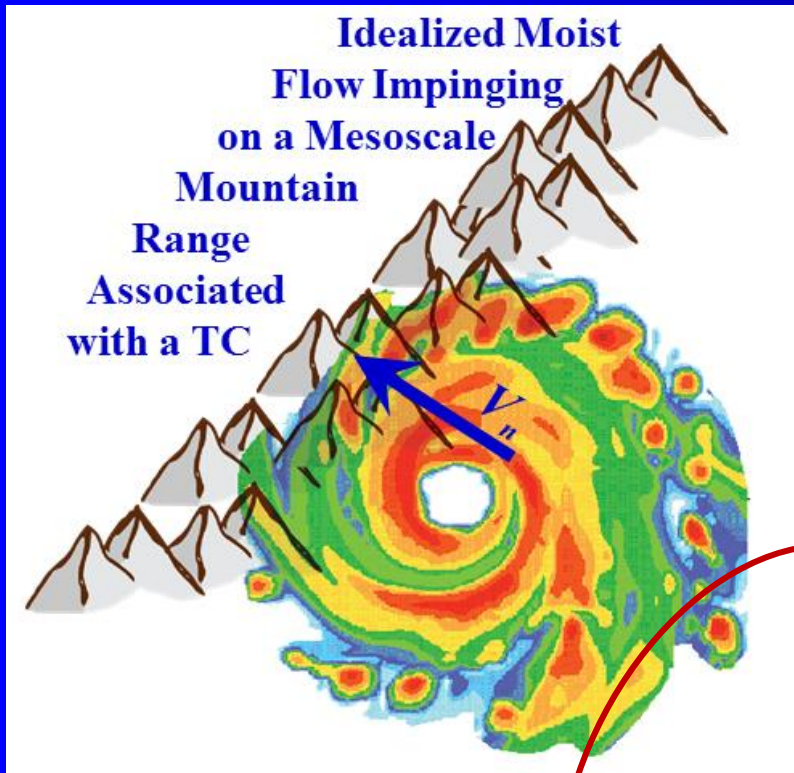
Large F_w
Small CAPE

(S.-H. Chen & Lin 2005 JAS)

[F_w is unsaturated Brunt-Vaisala frequency]

Q: What happens if the basic wind is associated with the eyewall or rainband?

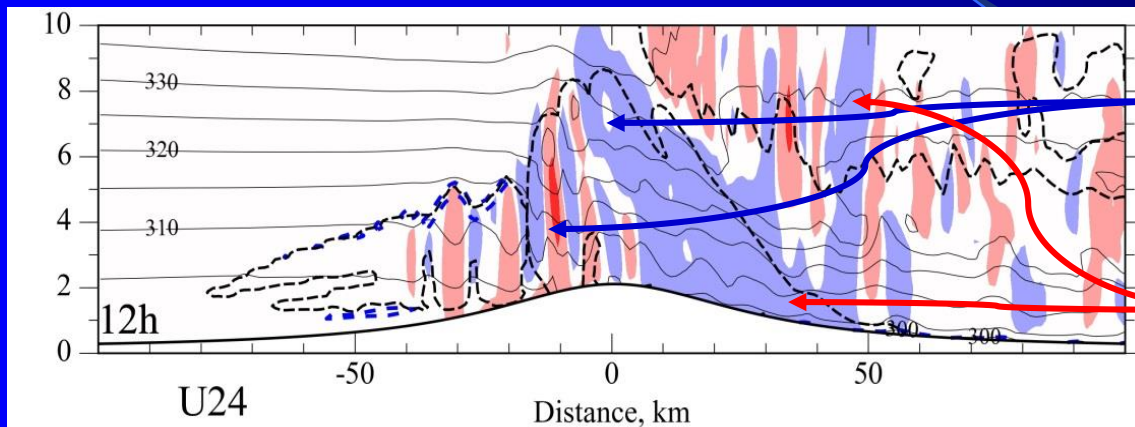
With strong wind, there exists a new flow regime (Regime IV)



Sever and Lin (2017 JAS)

The precipitating system is able to sustain strong wind with rainfall spilling over to the lee slope.

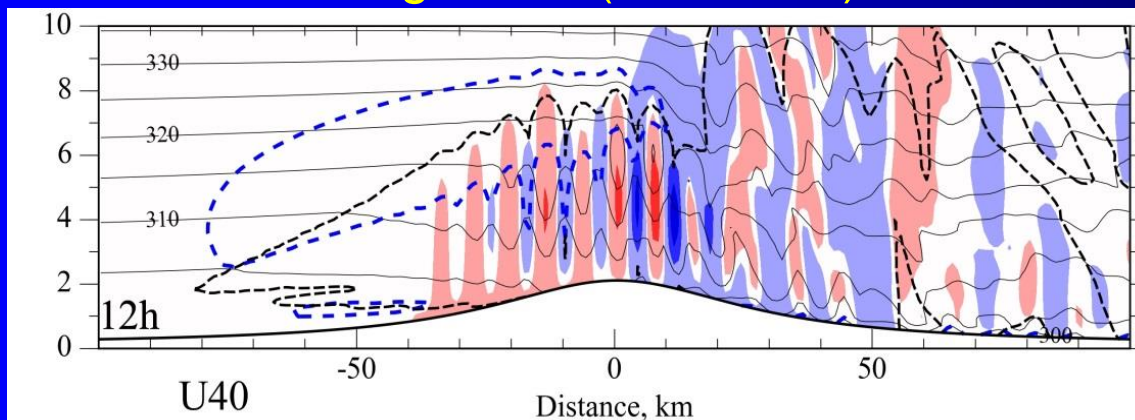
Regime III (9-36 m/s)



w & clouds

An orographic trailing-stratiform convective line?!

Regime IV (U > 36 m/s)



w & clouds

A new flow regime: Deep convection and heavy rainfall over both up- and down-slopes!

(Sever and Lin, 2017 JAS)

A.3 Common ingredients for heavy orographic rainfall

Following Doswell et al.'s (1996) ingredient approach:

Total rainfall (mm) = Rainfall rate (mm/h) x Duration of Precipitation (h)

$$P = RT$$

Since

$$R = \varepsilon(wq)$$

$$T = L_s / c_s$$

We have

$$P = \varepsilon(wq)(L_s / c_s)$$

P = total precipitation

R = rainfall rate

T = rainfall duration

ε = precipitation efficiency

wq = vertical moisture flux

L_s = hori. scale of precip system

c_s = precip system moving speed

Assume w can be linearly decomposed into

$$W = W_{env} + W_{oro}$$

For upslope rain, we assume

$$W_{oro} \approx U \partial h / \partial x \geq 0 \quad (2D)$$

$$W_{oro} \approx V \cdot \nabla h \geq 0 \quad (3D)$$

Therefore

$$P = \varepsilon (w_{env} + V \cdot \nabla h) q L_s / c_s$$

(Lin et al. 2001 WAF)

Based on

$$P = \varepsilon (V \cdot \nabla h + w_{env}) q L_s / c_s$$

in order to have large precipitation (P), we need any combination of key ingredients (Lin et al. 2001 WAF; Lin 2007):

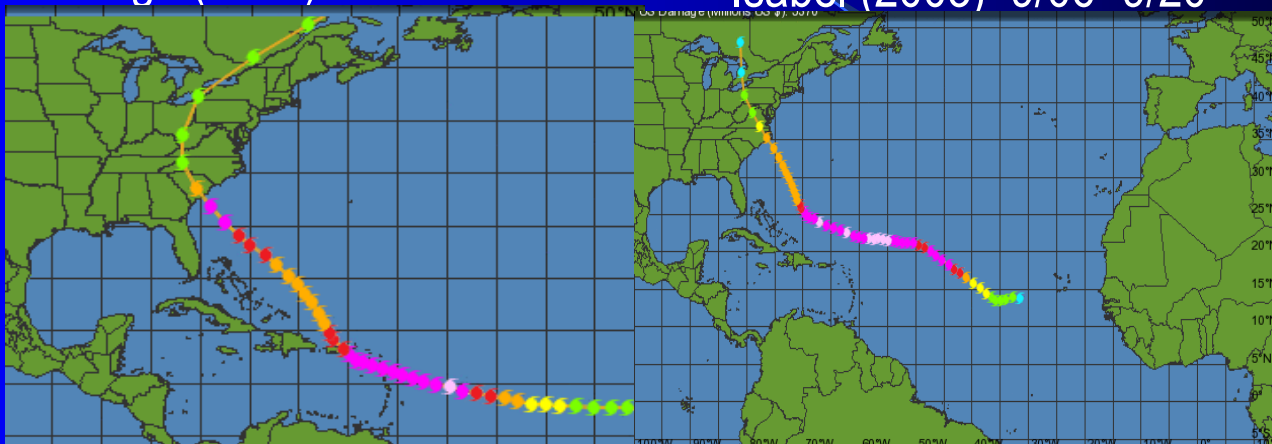
1. **High precipitation efficiency** (large ε)
2. **A low level jet (LLJ)**; large V)
3. **Steep mountain** (large ∇h or h/a)
4. **Strong synoptically forced upward motion** (large w_{env} ; e.g., conditionally unstable flow, low-level convergence, upper-level divergence)
5. **High moisture upstream** (large q or RH)
6. **A large precipitation system** (large L_s)
7. **A slowly moving precipitation system** (small c_s)

- The above common ingredient argument has been tested for several typhoon cases (e.g., Lin et al. 2001, Chiao and Lin 2003; Witcraft et al., 2005; Huang and Lin 2014)
- For Typhoon Morakot (2009), the key ingredients are high RH, slow movement, and orographic lifting (Huang and Lin 2014)
- Need to: (a) determine relative contributions from the common ingredients and (b) further understand the relations of w_{oro} and w_{env} .

Our recent WRF simulations indicate that orographic TC-rain asso. with Hurricanes Hugo (1989) and Isabel (203) over Appalachians are contributed from different ingredients.

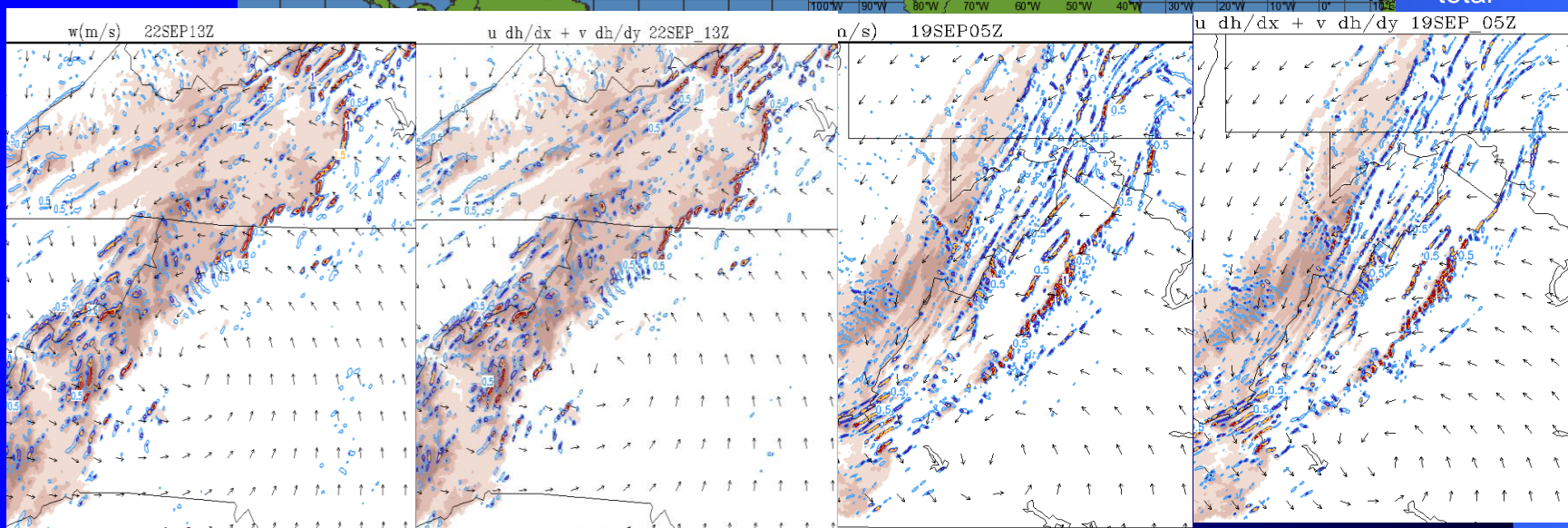
Hugo (1989) 9/10 - 9/25

Isabel (2003) 9/06- 9/20



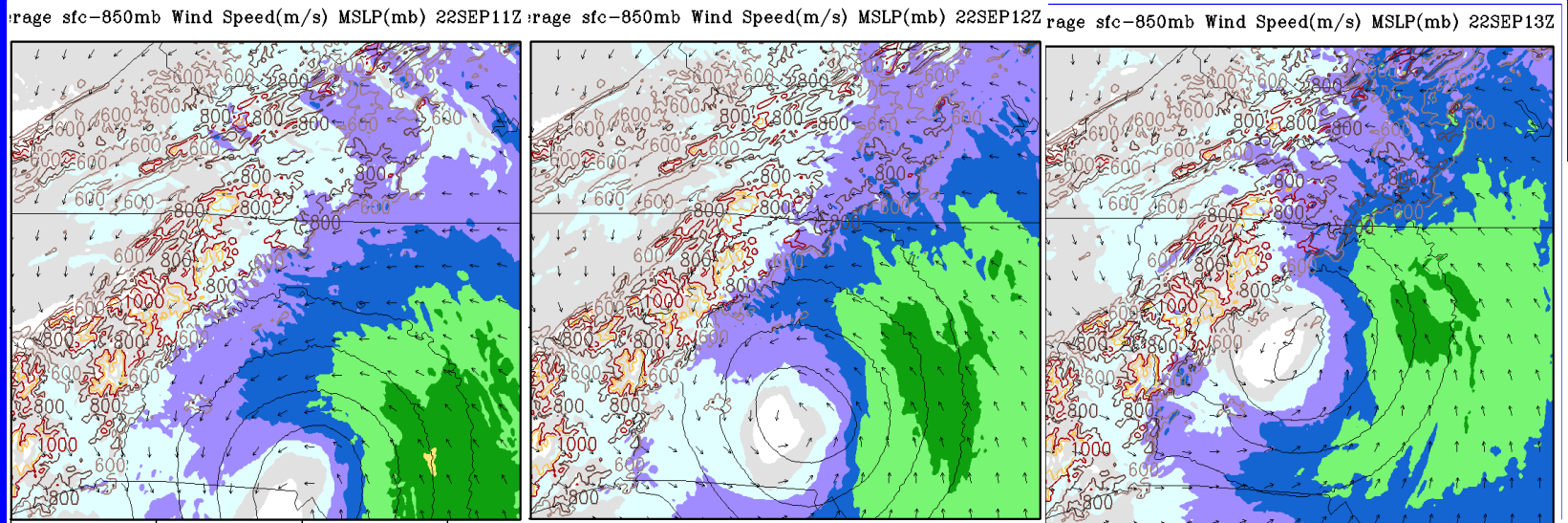
$W_{total} \sim W_{oro}$

$W_{total} \sim W_{oro}$

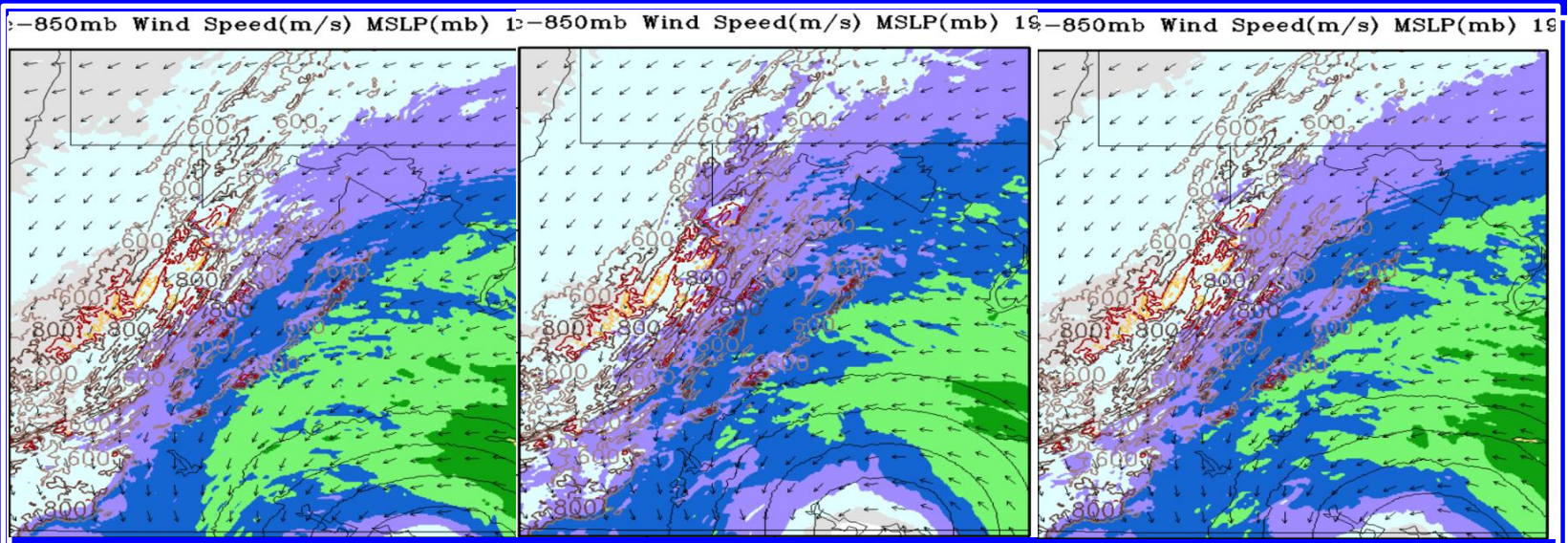


Surface-850mb LLJ (large $|V_H|$)

Hugo



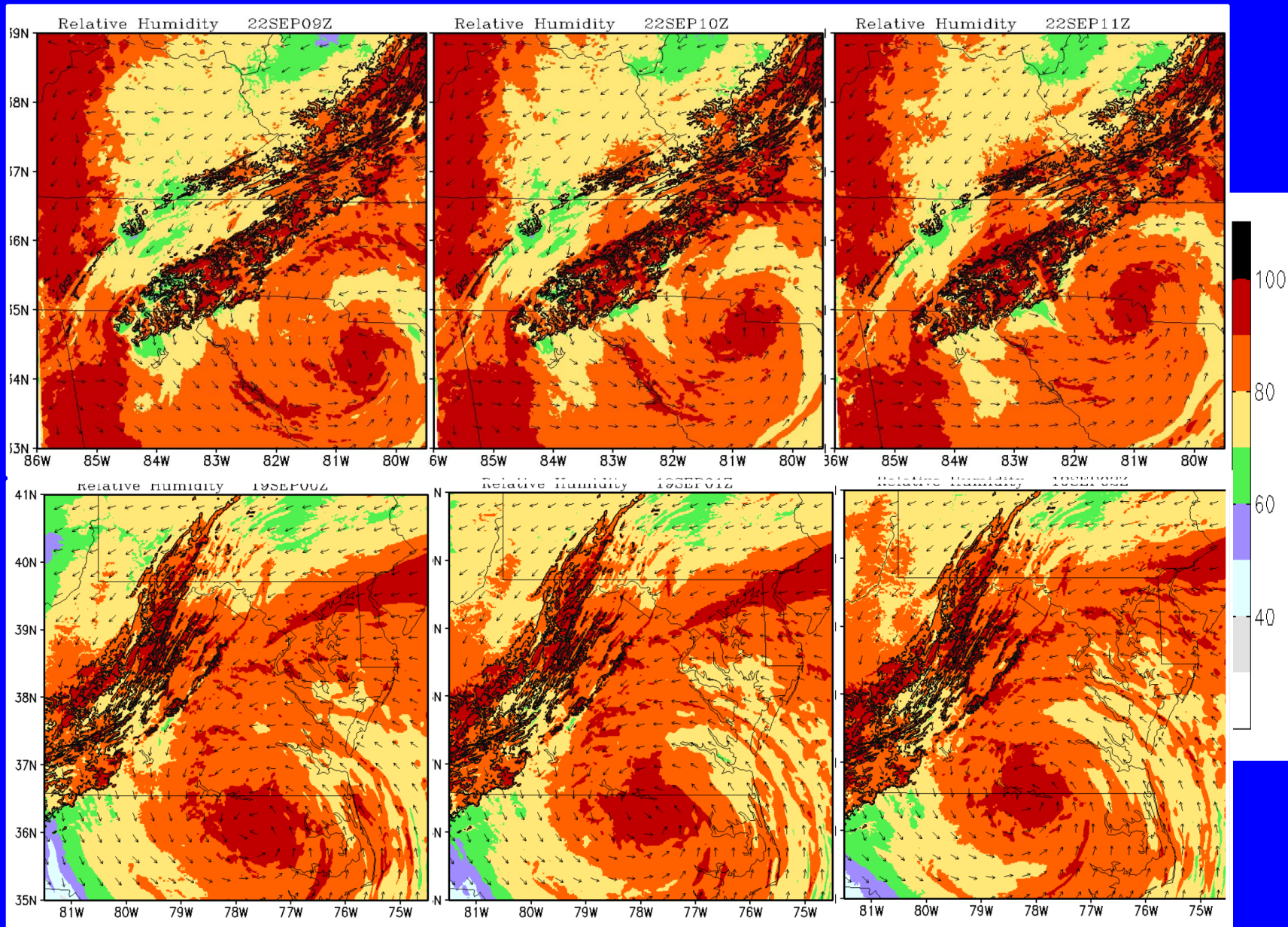
Isabel



There are plenty of moisture upstream: *high RH*

Hugo
~86%

Isabel
~80%



Key Ingredients for Hugo and Isabel are different

Hugo (1989)

From 9/ 21/12Z to 9/23/00Z

- $LLJ \sim 24\text{m/s}$ near sfc
- large $\mathbf{v}_H \cdot \nabla h$ ($\sim w_{oro}$)
- RH $\sim 86\%$
- $\mathcal{E} \sim 0.72$
- $c_s \sim 12.5$ m/s

Isabel (2003)

From 9/18/00Z to 9/20/00Z

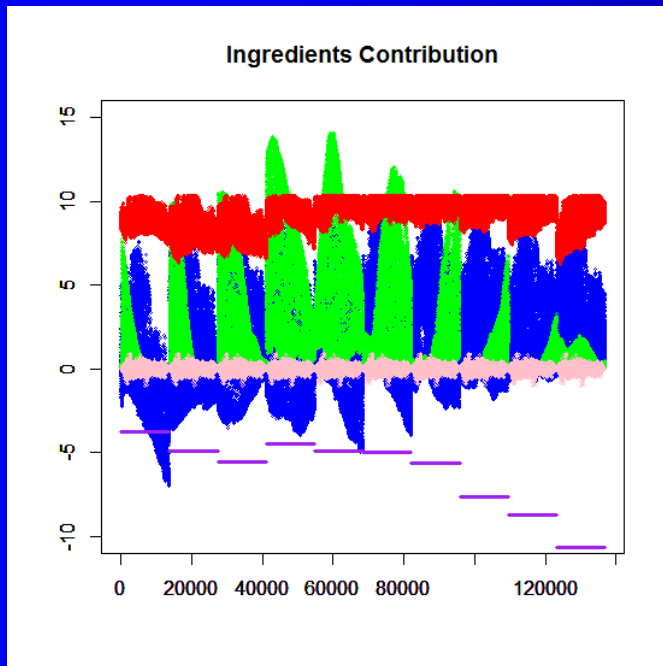
- $LLJ \sim 18\text{m/s}$ near sfc
- medium $\mathbf{v}_H \cdot \nabla h$ ($\sim w_{oro}$)
- RH $\sim 80\%$
- $\mathcal{E} \sim 0.97$
- $c_s \sim 8.8$ m/s

Isabel has more orographic rain due to:
slower movement and higher precip efficiency.

Applying a multiple linear regression and partial F-tests to determine relative contributions from the common ingredients to Isabel's (2003) rainfall

$$Y = \beta_0 + \sum_{i=1} \beta_i x_i$$

where Y is a vector of 3h rainfall mounts from 9/18/15Z – 9/19/18Z, x_1, \dots, x_7 correspond to 3h rainfall ingredients, and β_0, \dots, β_7 are the coefficients.



Red: RH

Purple: storm moving speed

Green: conditional instability

A.3 Development of an Index for Orographic TC Rain (TC-ORI)

Based on

$$P = \varepsilon \left(\frac{\rho_a}{\rho_w} \right) (V \cdot \nabla h + w_{env}) q_v \left(\frac{L_s}{\epsilon_s} \right)$$

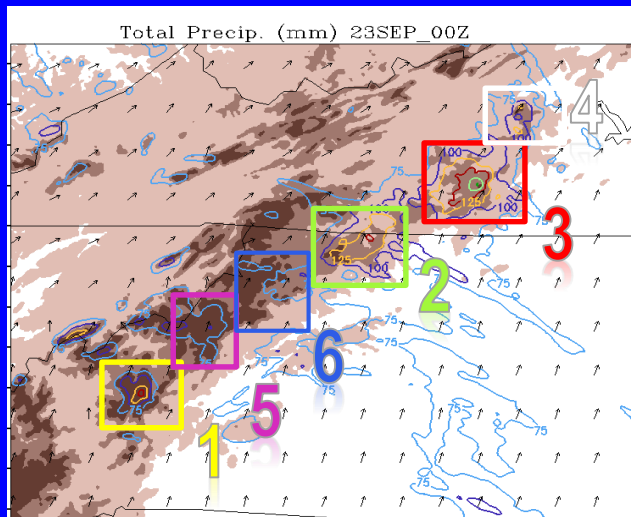
$\sim V_{\max N} \frac{dh}{dx}$ very small $\sim RH$ $\sim R$ $\sim U$

Rostom and Lin (2017) modified the index for heavy orographic rain for TC-rain (TC-ORI) to be

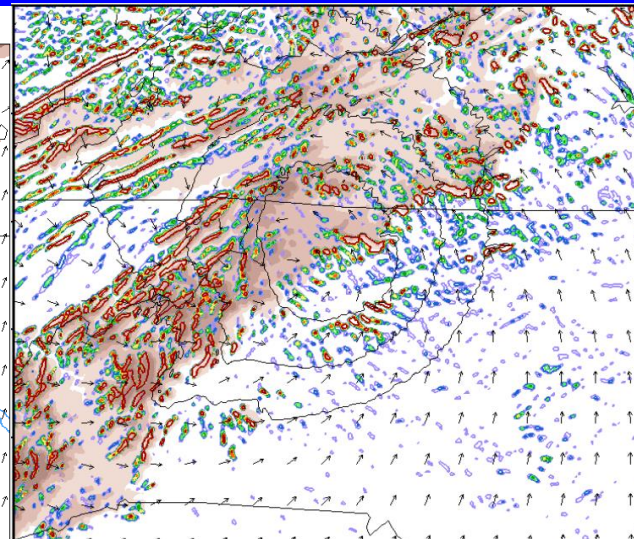
$$ORI = \left(V_{\max N} \frac{\Delta h}{\Delta x} \right) (RH) \left(\frac{R}{U} \right)$$

Model-generated ORI patterns are similar to the observed rainfall distribution

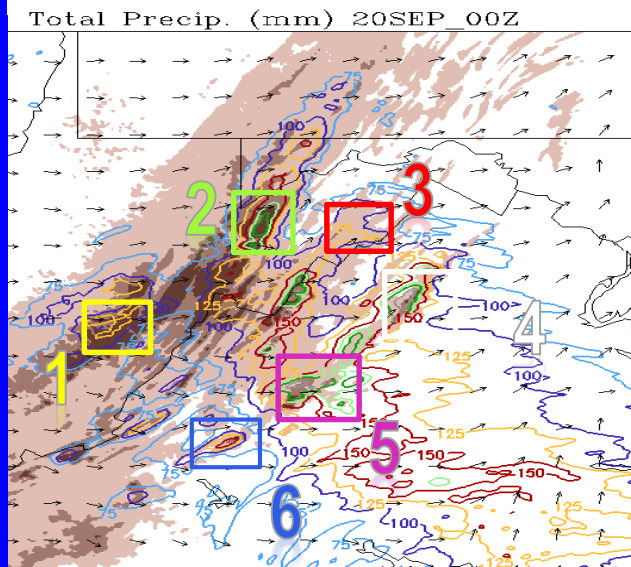
Hugo Rain



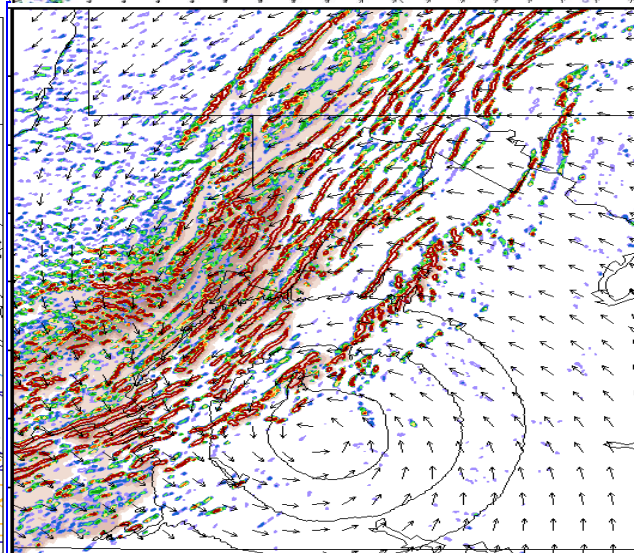
ORI at 9/22/14Z



Isabel Rain



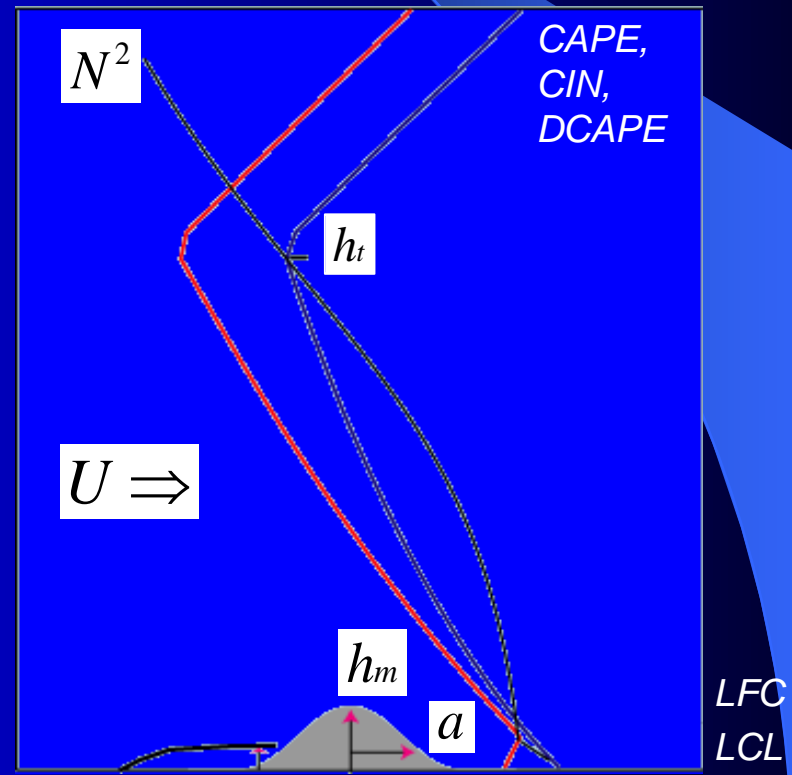
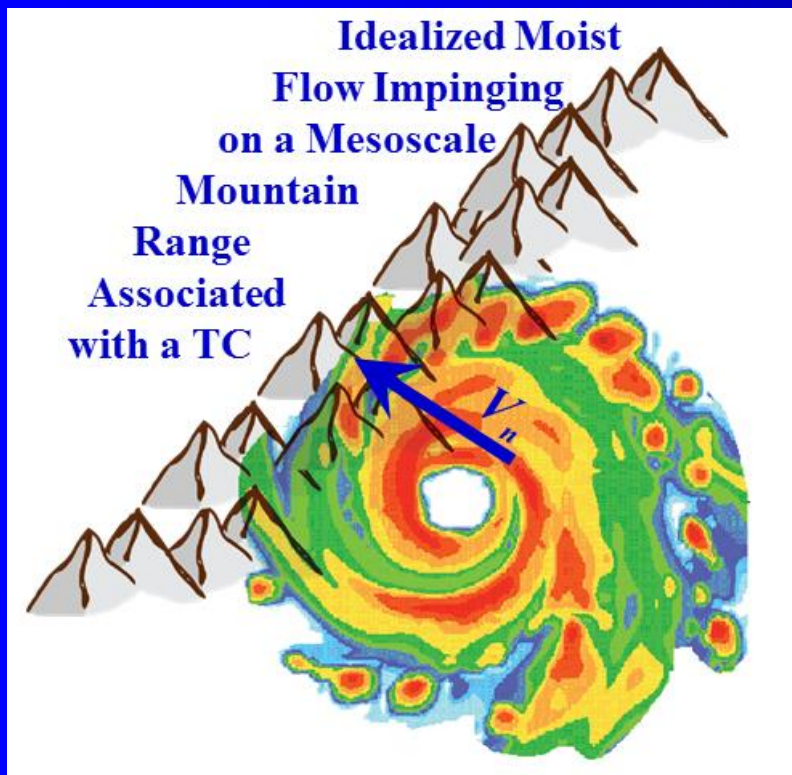
ORI at 9/19/06Z



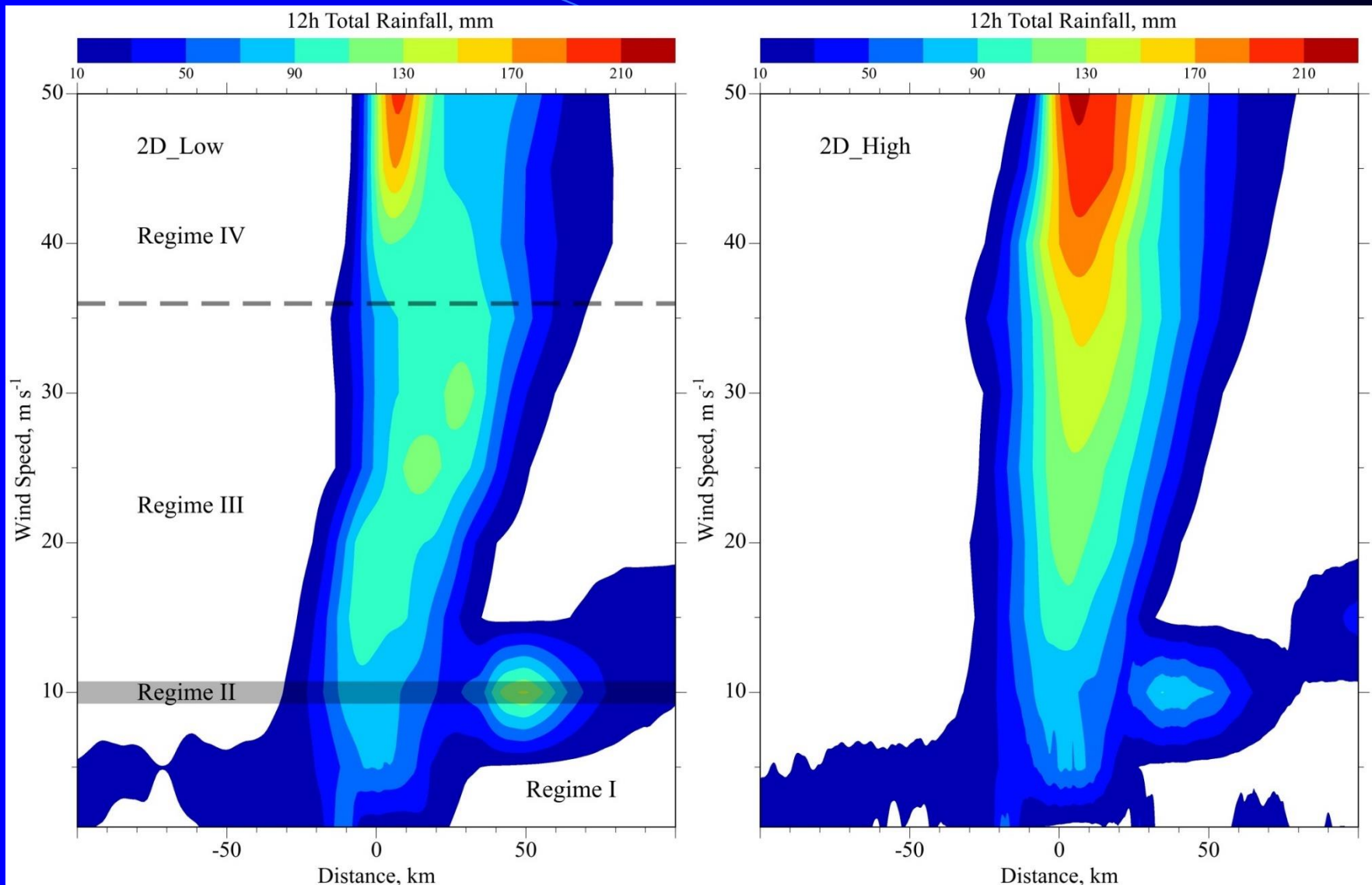
1 1.5 2 2.5 3 3.5 4 >4

A.4 Effects of Mechanical and Thermal Forcing on Orographic TC-rain in High Wind Regimes

Some fundamental dynamics in high wind regimes maybe understood by making idealized simulations.

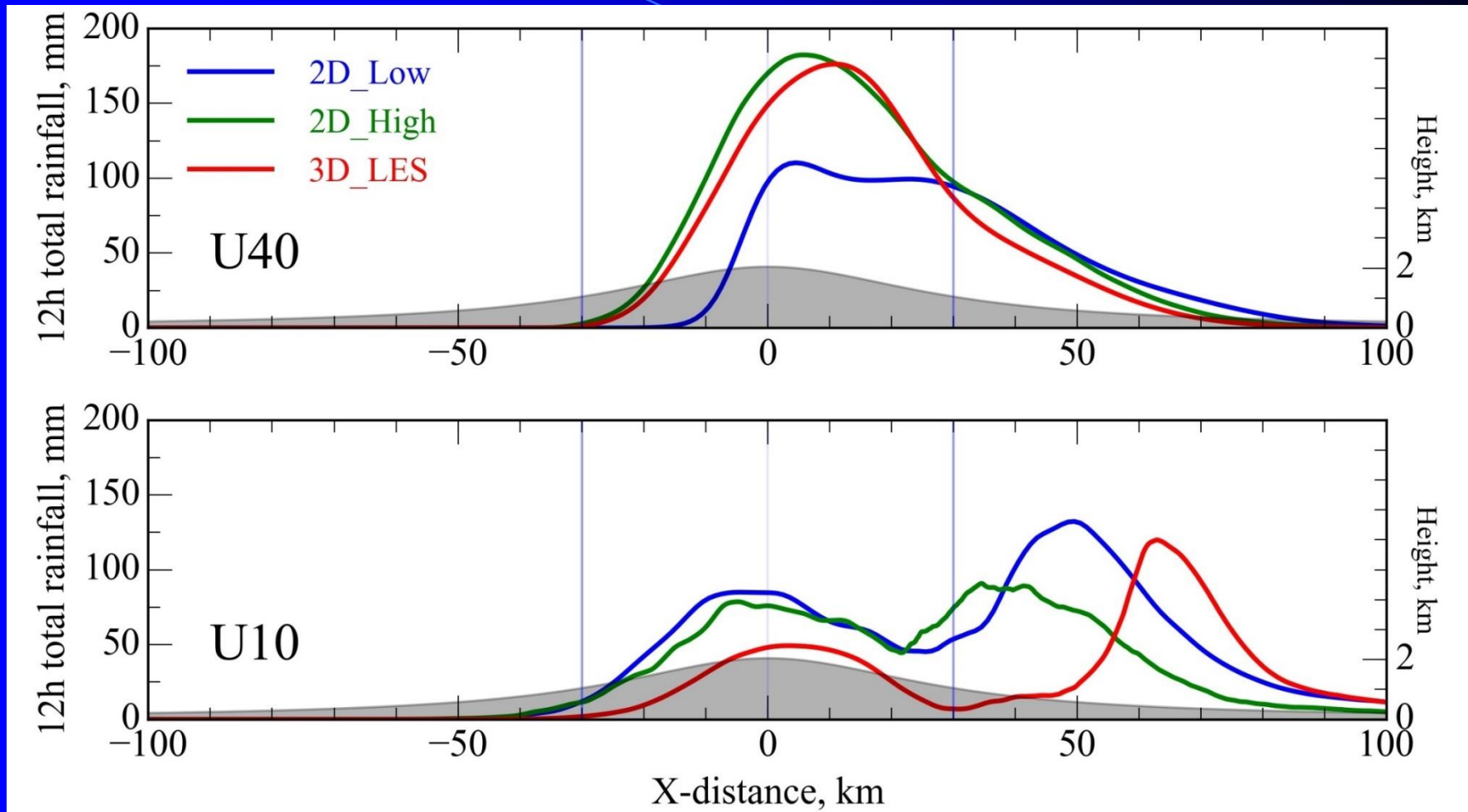


Rainfall amount increases dramatically with higher grid resolution



2D_Low: $\Delta x = 1\text{km}$, $\Delta z \sim$ from 250m, $\Delta t = 1\text{s}$; $L_x = 1000\text{ km}$, $h=2\text{km}$, $a=30\text{km}$;
2D_High (3D LES): $\Delta x = \Delta y (= \Delta z) = 100\text{ m}$, $\Delta t=\text{adaptive} \sim 1.3\text{s}$; $L_y = 10\text{ km}$.

Rainfall distributions at 12 h



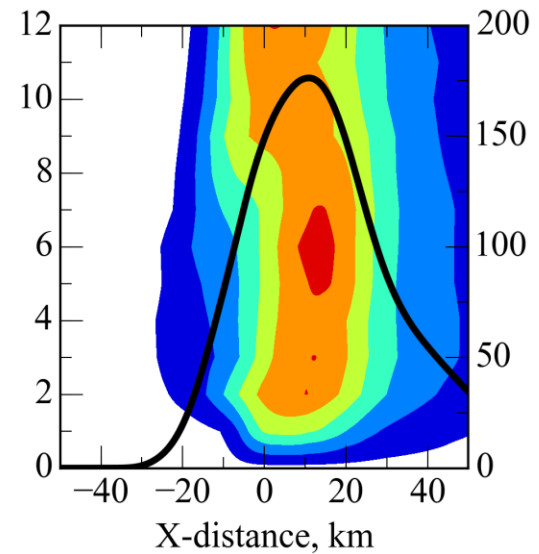
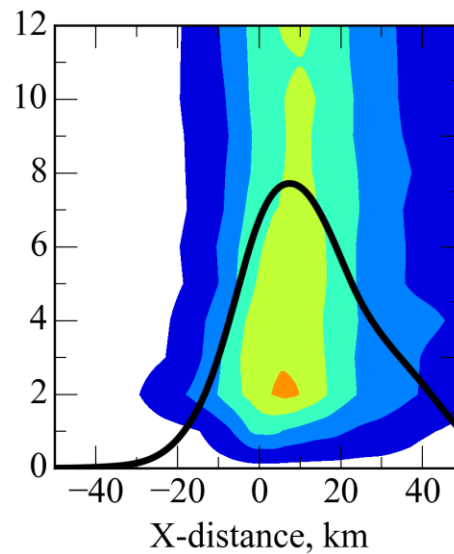
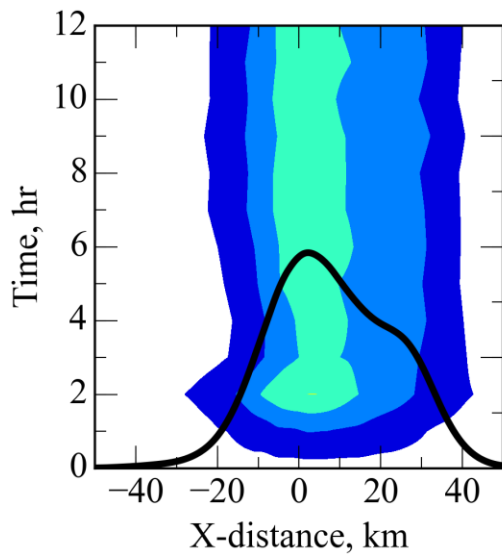
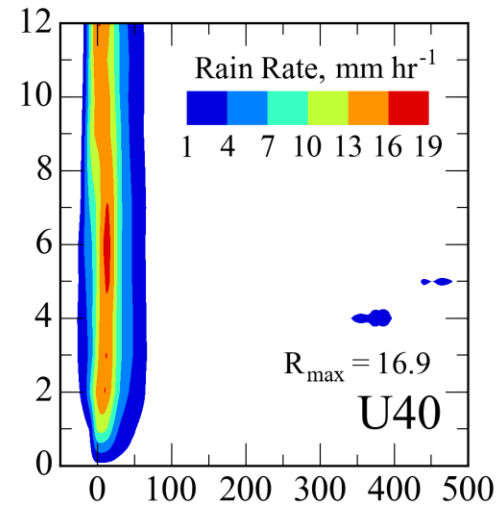
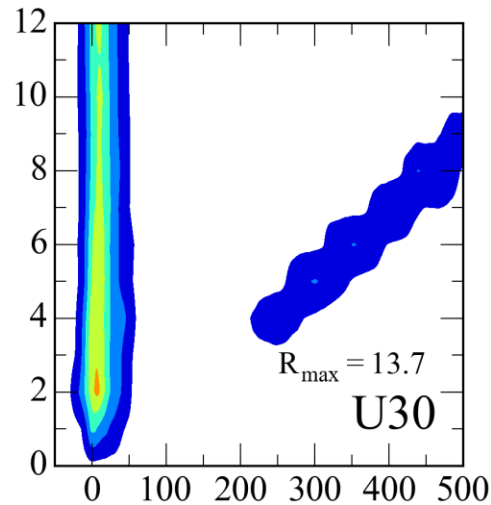
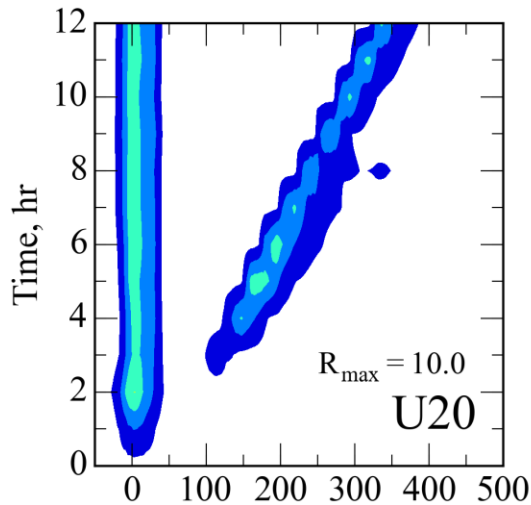
- **2D_High** and **3D_LES** show a similar distribution pattern and amount for high wind.
- For low wind regimes, both 2D_High and 2D_Low overpredict the rainfall amount.

Rainfall rates in Hovmöller Diagram

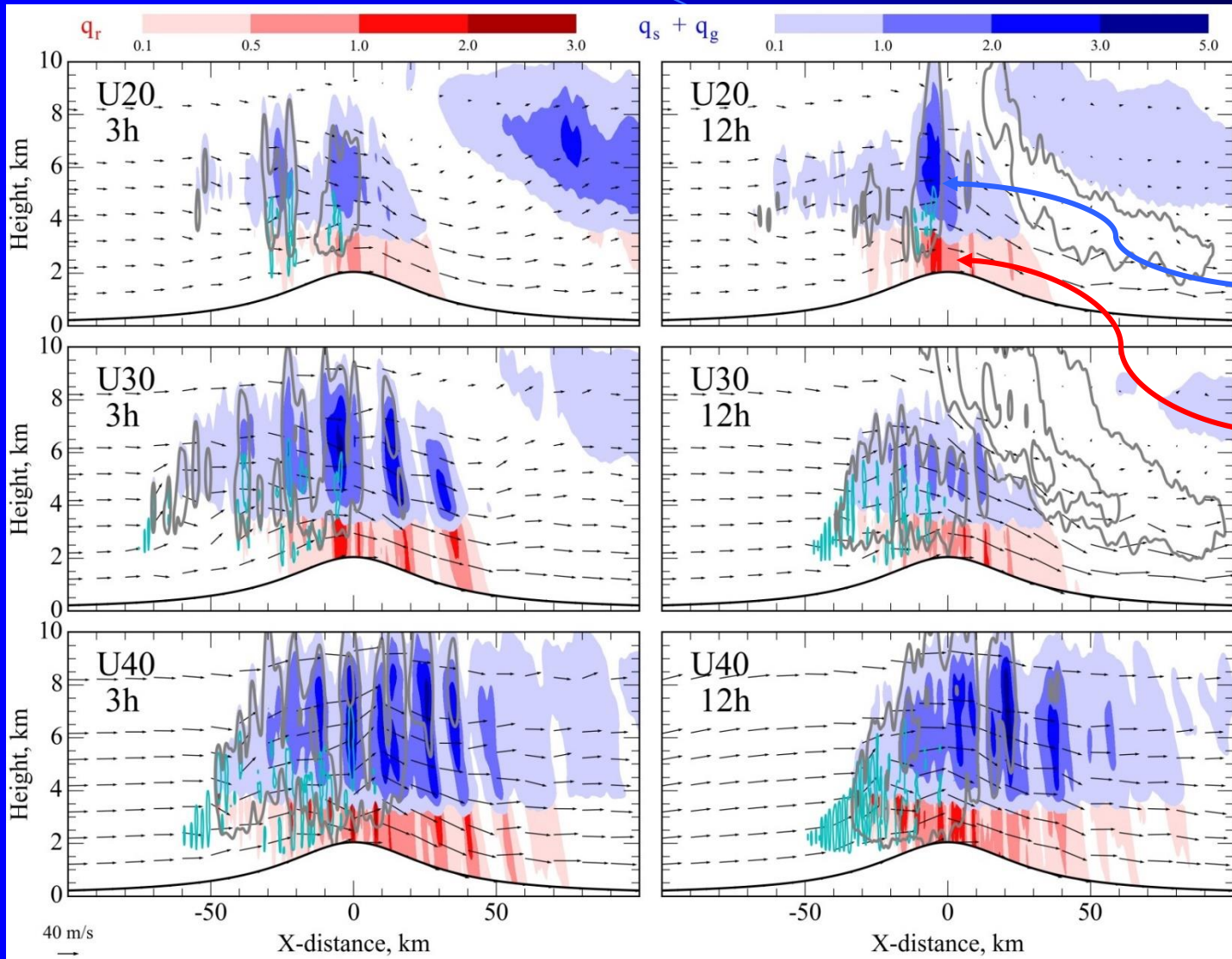
U=20 m/s

U=30 m/s

U=40 m/s



Hydrometeor, wind and turbulence fields



Rainfall weakened by gravity waves.

$q_s + q_g$
(snow + hail)

q_r (rain)

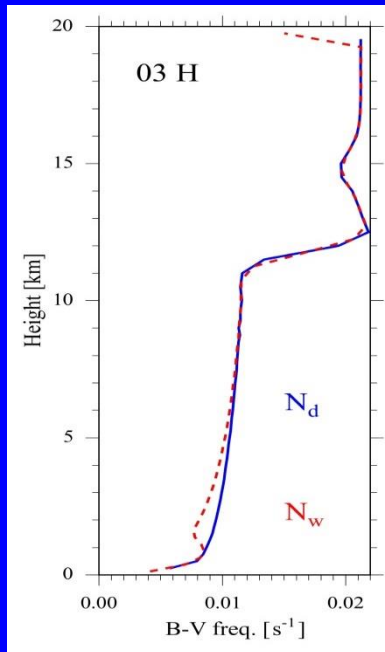
Evanescent flow regime
($a/U < 2\pi/N_w$)

Allows deep convection to develop over lee slope.

Regime Transition in U30 – U40 Range

- Dynamical response of the system transitions from vertically propagating to evanescent waves in Regime IV ($U > 36$ m/s).

at $x = -200$ km



$$\frac{d^2 \hat{w}}{dz^2} + (l_w^2 - k^2) \hat{w} = 0 \quad \text{(2D Taylor-Goldstein Eq. in Fourier Space)}$$

$$\hat{w}(k, z) = \hat{w}(k, 0) e^{i \sqrt{l_w^2 - k^2} z} \quad \text{for } l_w > k \quad \text{(vertically propagating waves)}$$

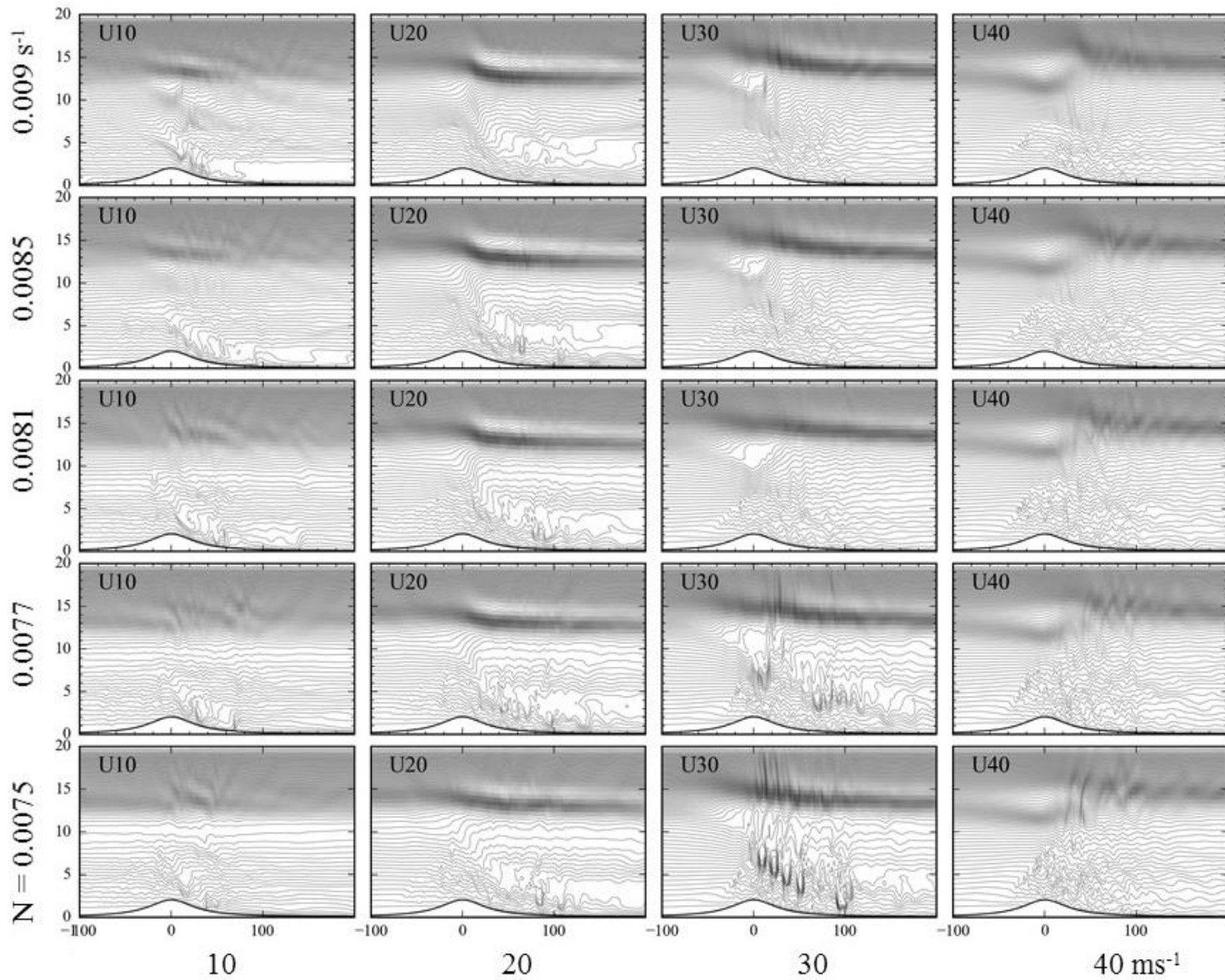
$$\hat{w}(k, z) = \hat{w}(k, 0) e^{-\sqrt{k^2 - l_w^2} z} \quad \text{for } l_w < k \quad \text{(evanescent flow)}$$

$$\text{Scorer parameter, } l_w \approx \frac{N_w}{U}; \quad k = \frac{2\pi}{a} = 2.1 \times 10^{-4} \text{ m}^{-1}$$

$$l_w = (3.75, 2.08, 1.88) \times 10^{-4} \text{ m}^{-1} \text{ for } U_{20}, U_{36}, \text{ and } U_{40}$$

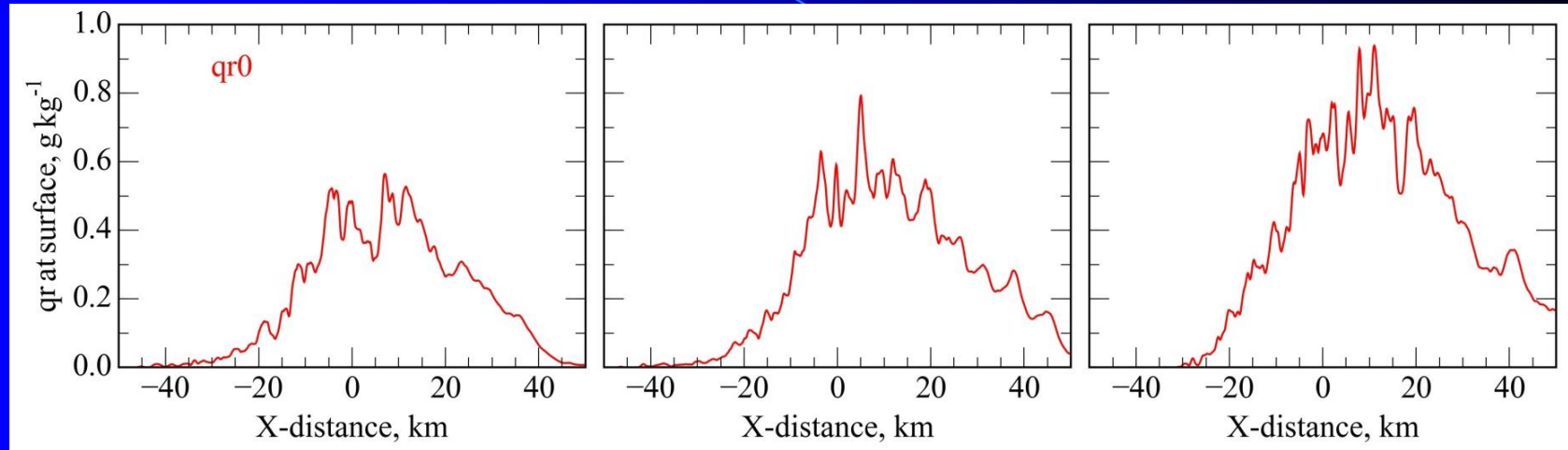
In other words, **horizontal advection** plays a more dominant role than **buoyancy** when $l < k$ (or $U > 2\pi N_w a$).

Evolutions of Flow fields (θ)

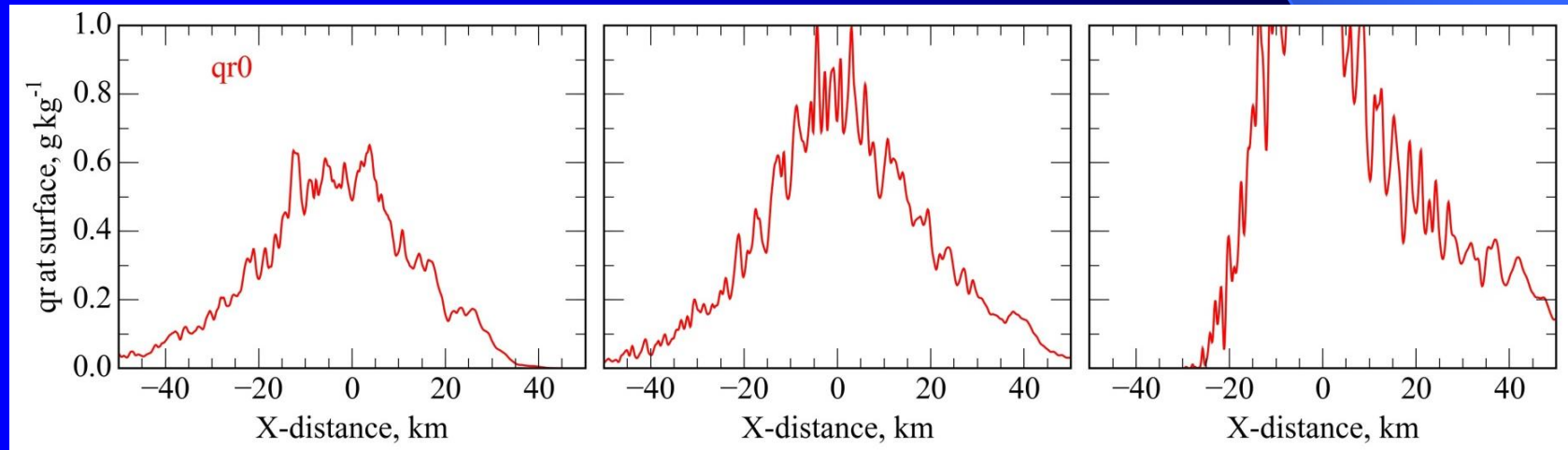


Our recent simulations indicate that the Low-CAPE flow produce more rain than the High-CAPE flow

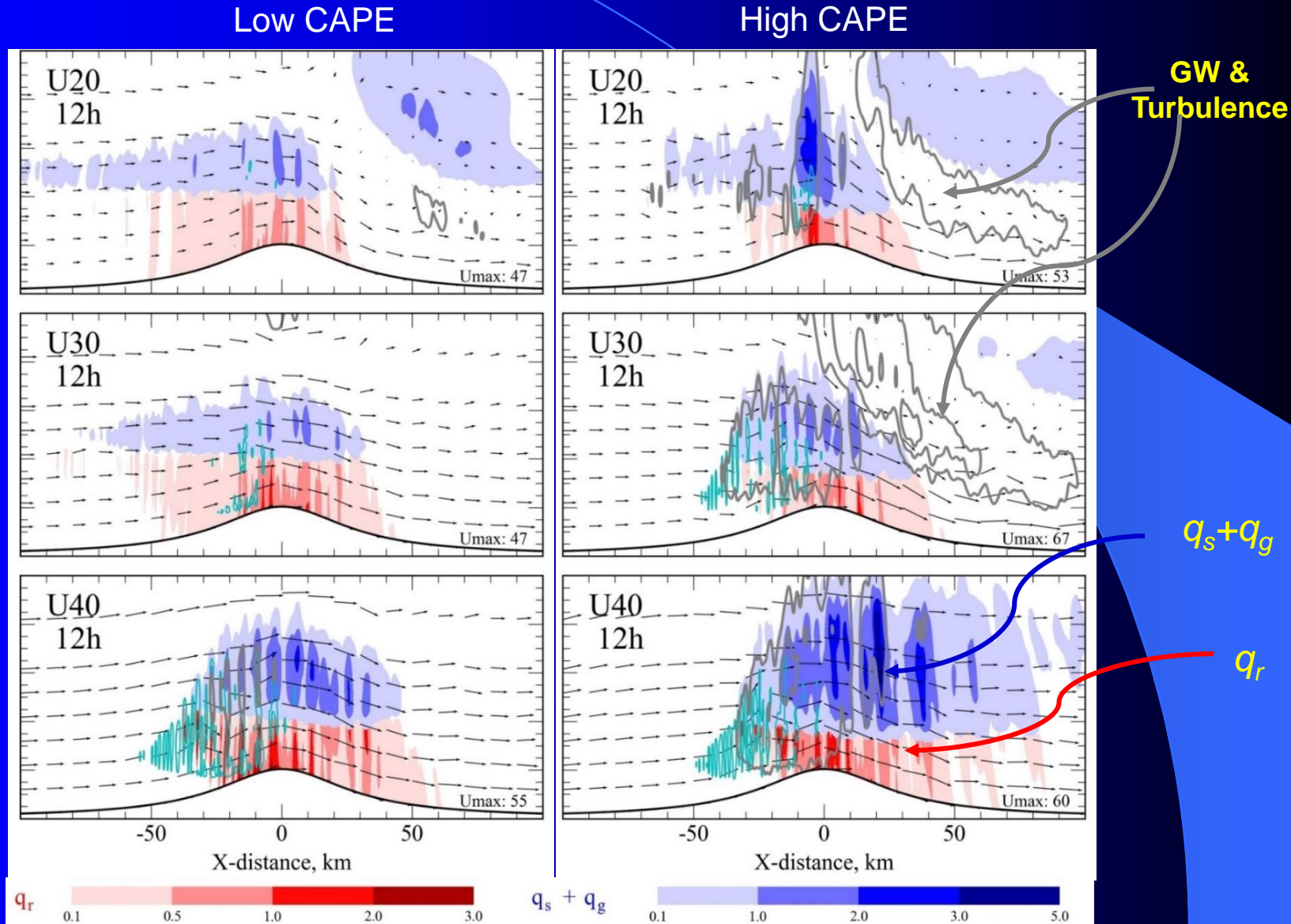
High
CAPE



Low
CAPE



(a) The High-CAPE flow does produce stronger and deeper convective cells and more hydrometeors in the middle and higher troposphere.

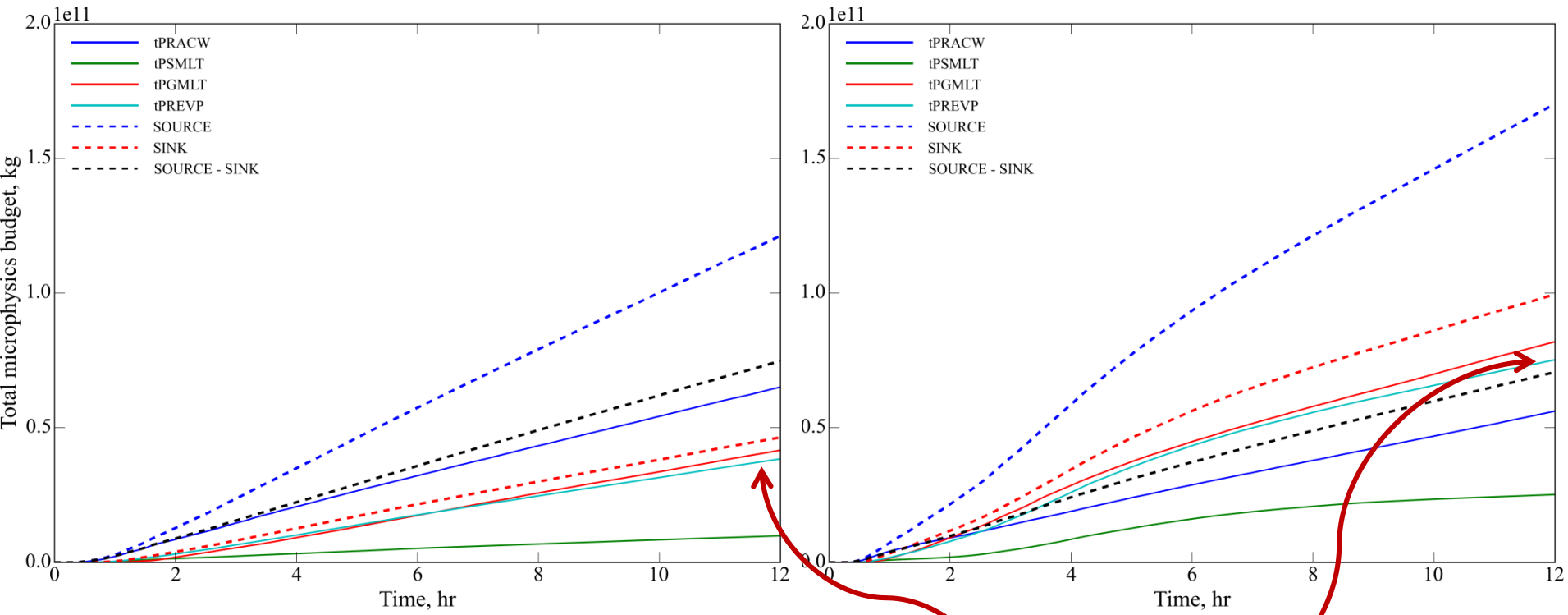


(b) For higher wind regimes, even though the High CAPE flow produces larger rain, the evaporation is much larger. Thus, the precipitation on the ground is less.

Dominant microphysical processes of q_r at $U = 40 \text{ m s}^{-1}$

Low CAPE

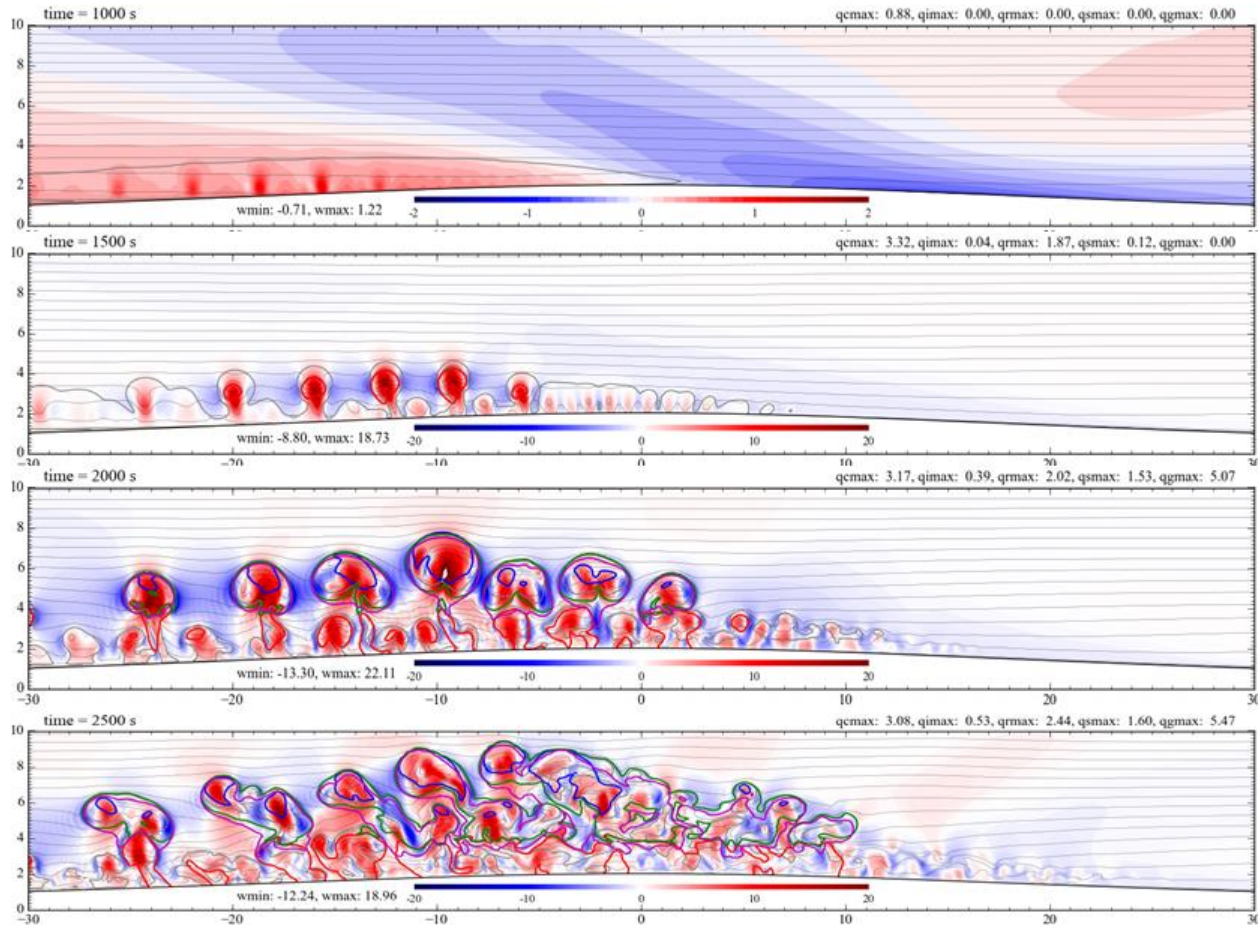
High CAPE



PRACW: Accretion of cloud water by rain
PSMLT: Melting of snow to form rain

PGMLT: Melting of graupel to form rain
PREVP: Evaporation of rain

How much do you really know about convective system is initiated in the model? Well, probably not much!



A.5 Conclusions (Part A)

- The key ingredients for orographic TC-rain have been further examined for Hurricanes Hugo and Isabel.
- The ORI is modified for orographic TC-rain:

$$ORI = \left(V_{\max N} \frac{\Delta h}{\Delta x} \right) (RH) \left(\frac{R}{U} \right)$$

- The ORI needs to be tested for more TC-rain cases.
- Effects of turbulence and gravity waves on orographic TC rain need to be further explored.
- Effects of mechanical and thermal forcing on orographic TC rain need to be further studied.

B.2 Mechanisms Proposed in Previous Studies

Based on previous studies, the following effects or mechanisms have been proposed to explain the upstream track deflection:

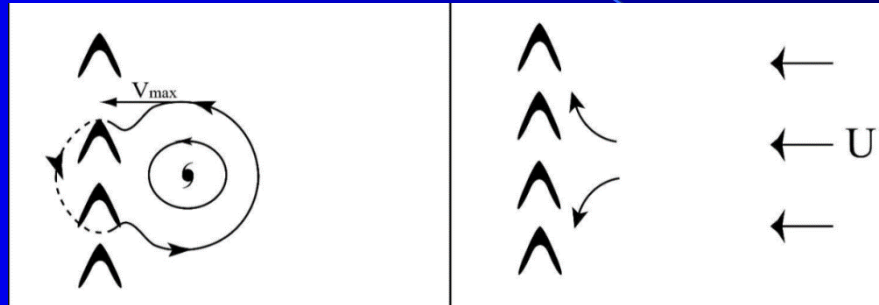
- (1) **cyclonic circulation effect** (e.g., Chang 1982; Bender et al. 1987)
- (2) **orographic blocking in response to various factors** (e.g., Yeh and Elsberry 1993a,b; Lin et al. 2005)
- (3) **channeling effect** (e.g., Lin et al. 1999; Jian and Wu 2008; Huang et al. 2011)
- (4) **asymmetric latent heating effect** (e.g., Chan et al. 2002; Hsu et al. 2013; Wang et al. 2013; Tang and Chan 2013, 2014; Lin et al. 2016)
- (5) **northerly asymmetric flow steering effect** (Wu et al. 2015)
- (6) **effect of terrain-induced beta gyres** (e.g., Tang and Chan 2013, 2014)
- (7) **effect of approach angle and landing location** (e.g., Lin and Savage 2011; Tang and Chan 2014; Liu et al. 2016).

A more fundamental approach is needed to build a unified theory for orographic influence on TC upstream, passing over the mountain and movement on the lee.

B.3 Theoretical Consideration

Conceptually, orography may affect TC tracks in two ways:

on TC vortex circulation

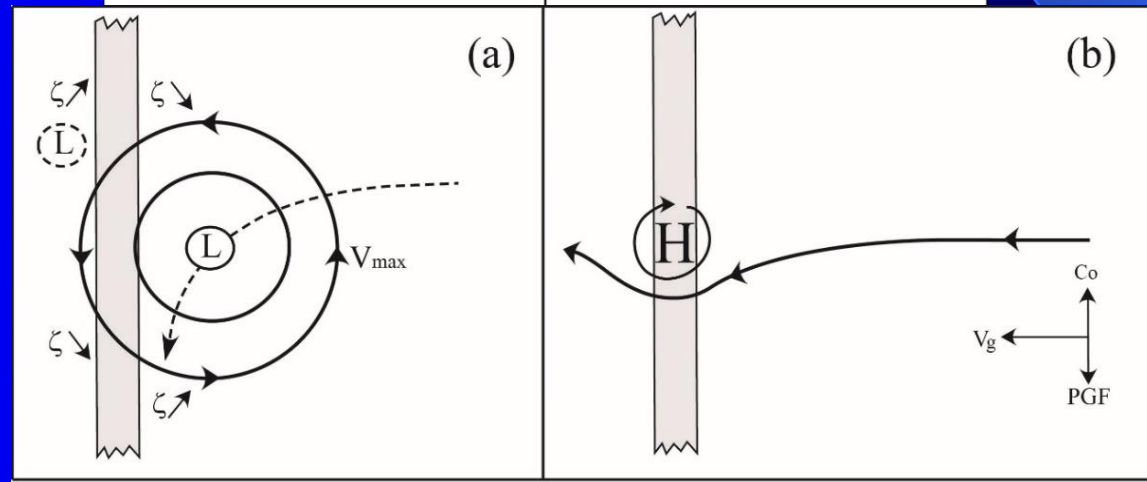


on basic flow

(Lin et al. 2005)

on TC vortex circulation

$$V_{max}/Nh$$



on basic flow

$$U/Nh$$

Lin et al. (2005), Lin (2007, *Meso. Dyn.*, Cambridge)

Q: Does linear superposition work? Do they work in moist atmosphere?

Q: What are the control parameters?

Lin et al. (2005) proposed that a passive vortex track becomes discontinuous when a combination of small V_{max}/Nh , U/Nh , R/L_y , U/fL_x , and V_{max}/fR , R/L_y , U/fL_x , V_{max}/fR , and large h/L_x occurs.

- U/Nh : basic-flow Froude number (controls dir. of deflection)
- V_{max}/Nh : vortex Froude number (controls degree of deflection)
- h/L_x : steepness of the mountain
- R/L_y : nondimensional cyclone scale
- U/fL_x : basic-flow Rossby number
- V_{max}/fR : vortex Rossby number

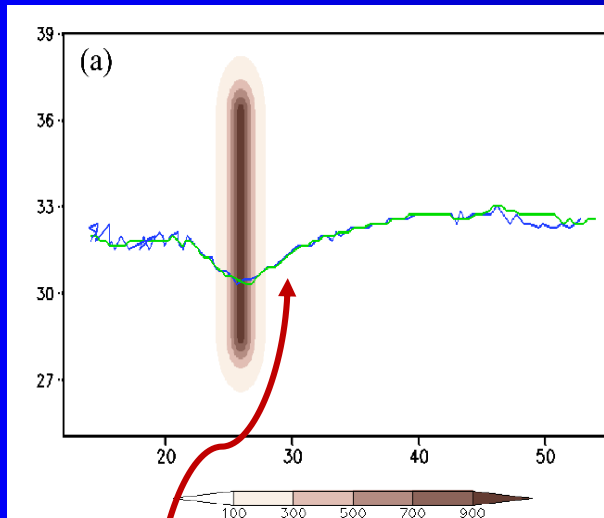
Q: Do they work in a moist atmosphere?

- Before sorting out the dominant control parameters, we need a better understanding of mechanisms for track deflection in a simple environment.
- Rostom and Lin (2015 WAF) found that V_{max}/Nh and V_{max}/fR play major roles in track discontinuity of extratropical cyclones over Appalachians.

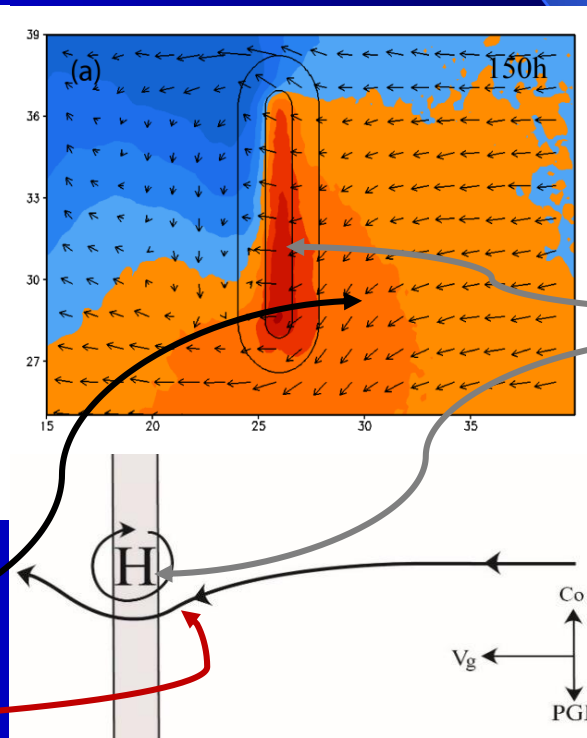
Upstream of the mountain

- The easterly basic flow is decelerated due to orographic blocking
- The flow becomes subgeostrophic which advects the TC to the southwest
- It is analogous to the advection of a point vortex embedded in a flow.

CNTL Case



NoTC Case



900 mb height

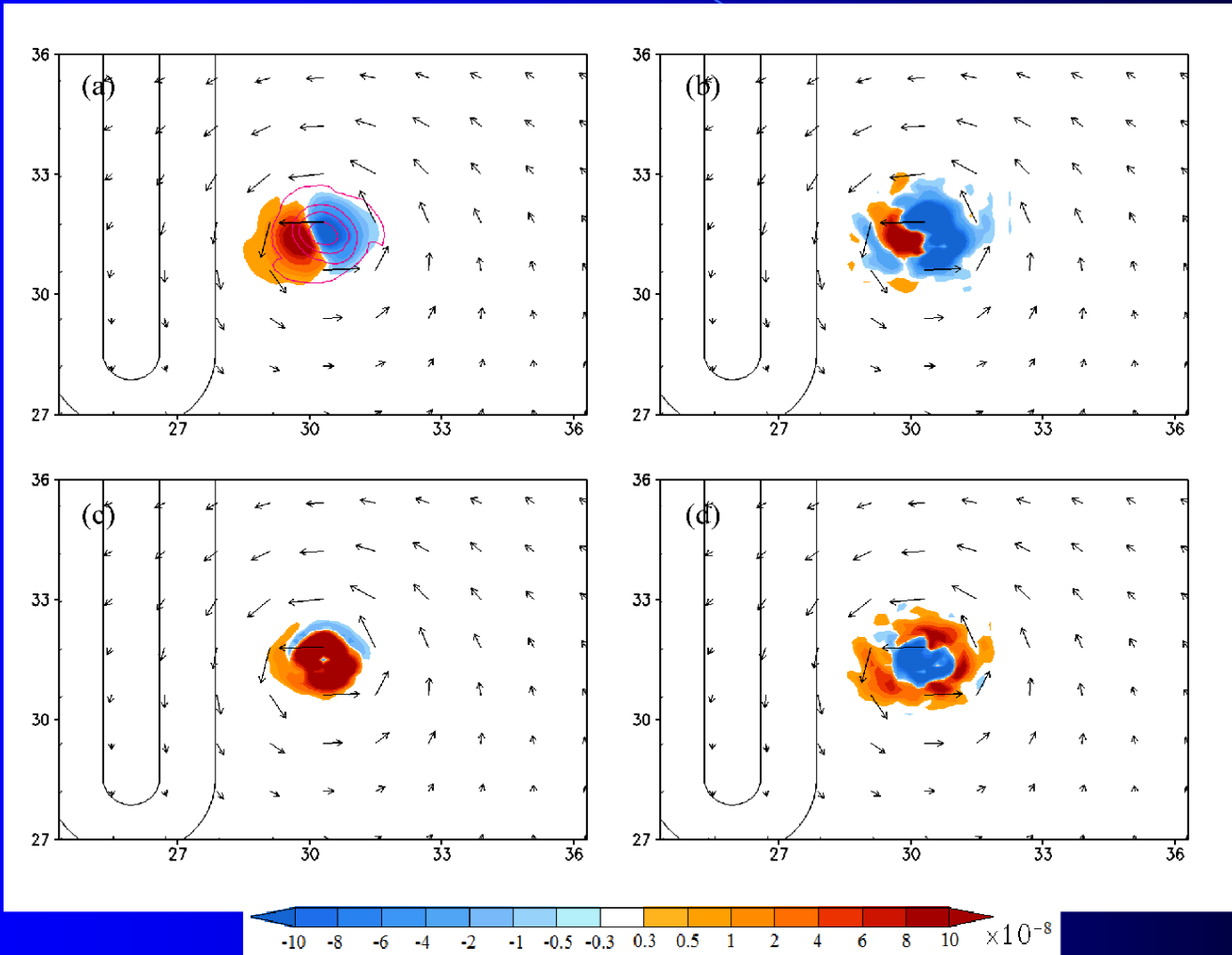
Mountain-induced High

deflected to south upstream

Upstream of the mountain (150 h), VT is dominated by the vorticity advection

VT

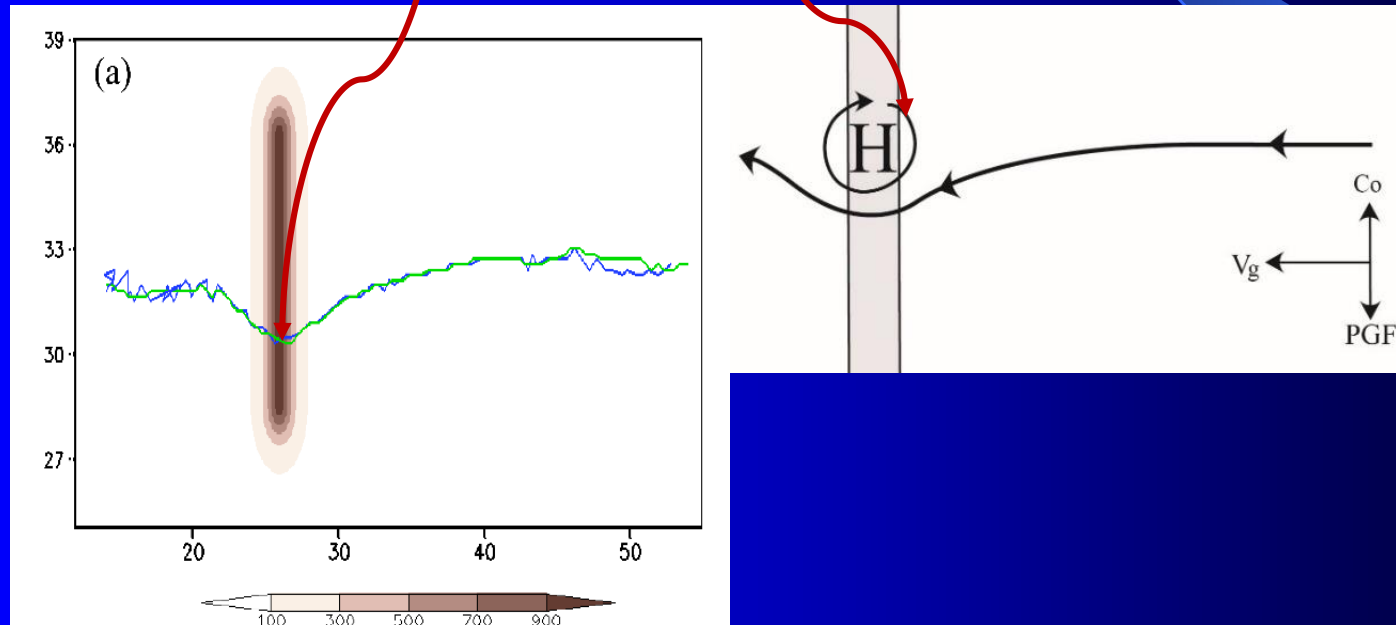
ζ_{advec}



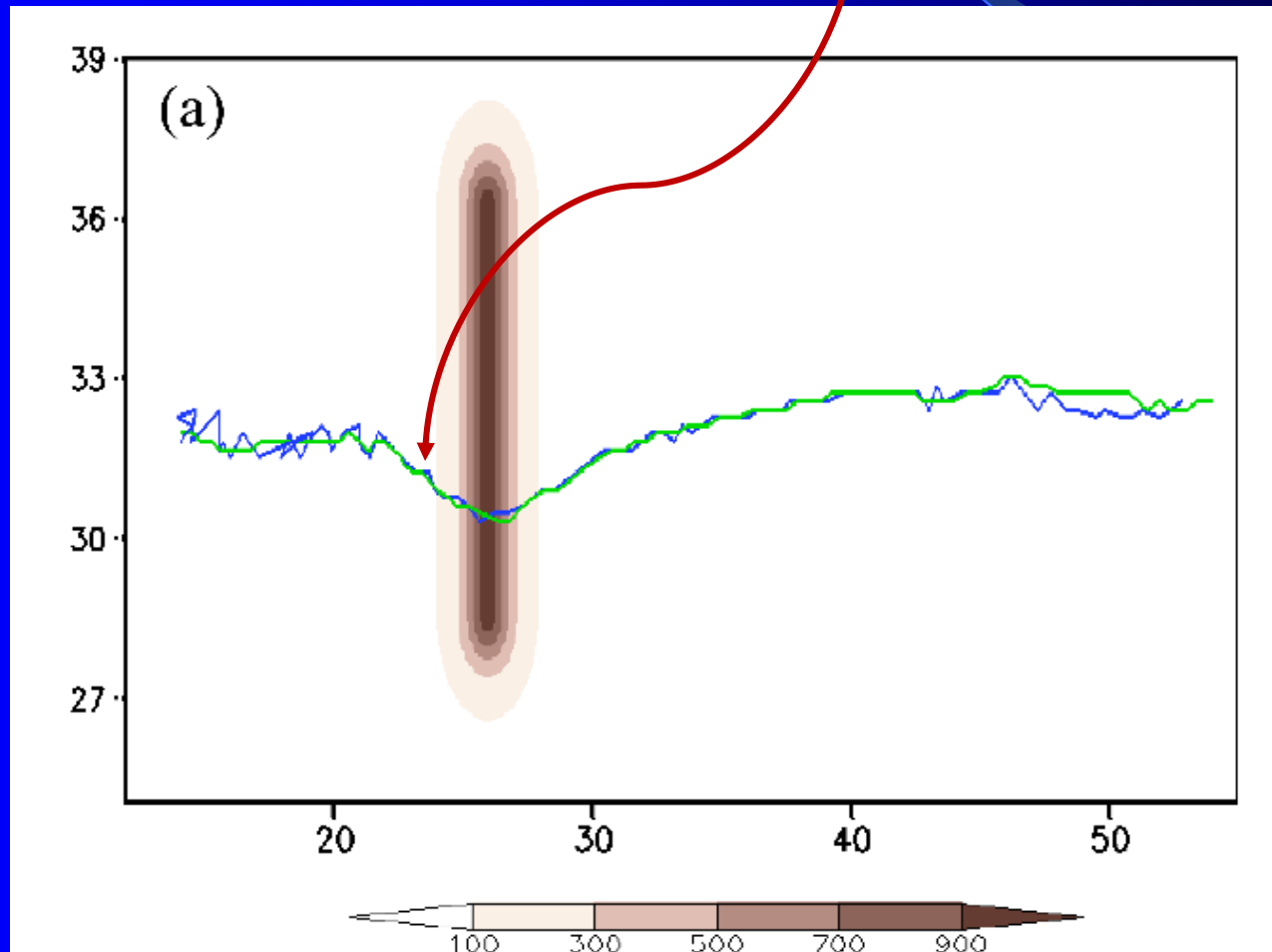
ζ_{str}

Res

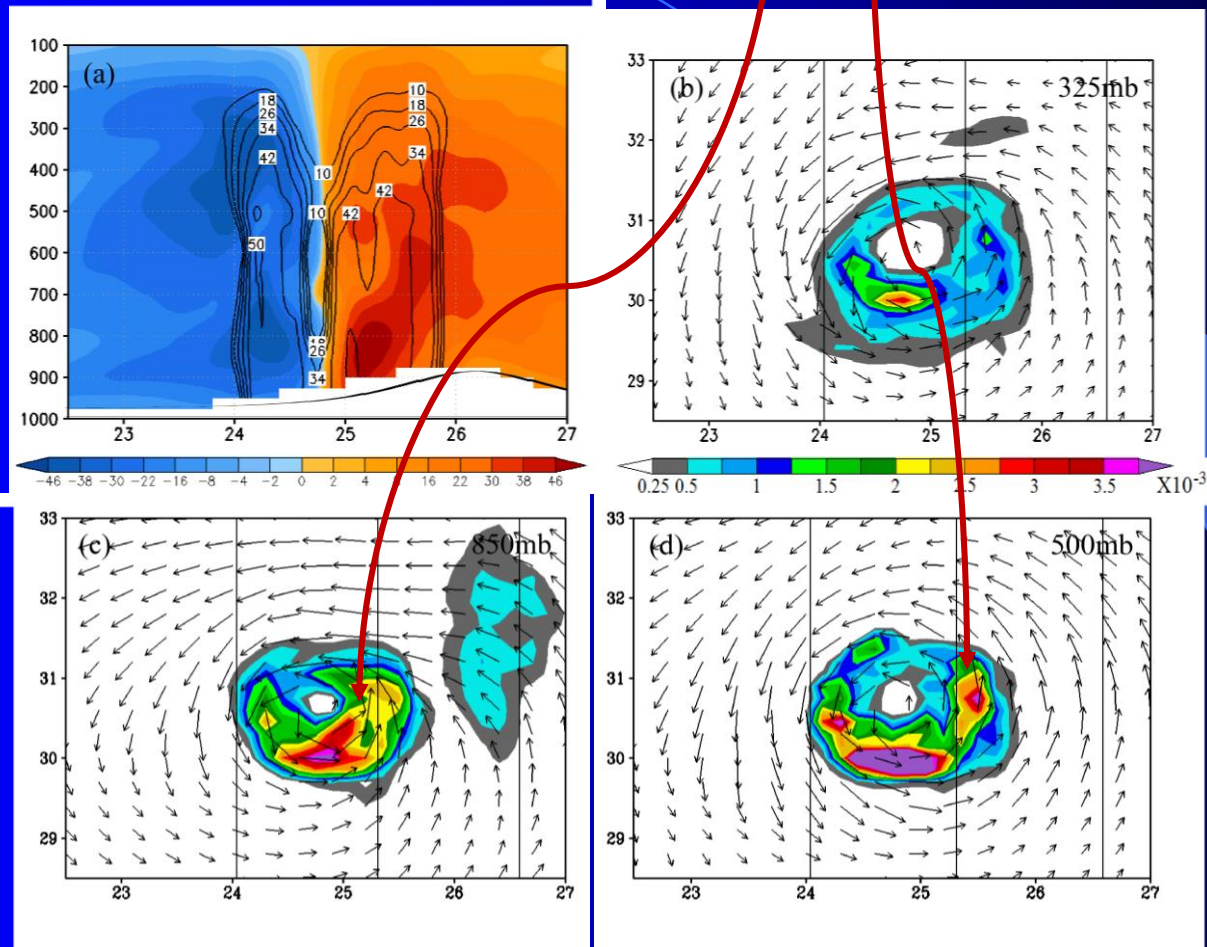
The TC passes over the mountain anticyclonically, mainly steered by the mountain-induced high.



Over the lee slope and downstream of the mountain, **the northwestward movement is enhanced by asymmetric diabatic heating**, making the turning more abruptly.



Over the lee slope and downstream of the mountain, the **NWward movement is enhanced by asymmetric diabatic heating**, making the turning more abrupt.

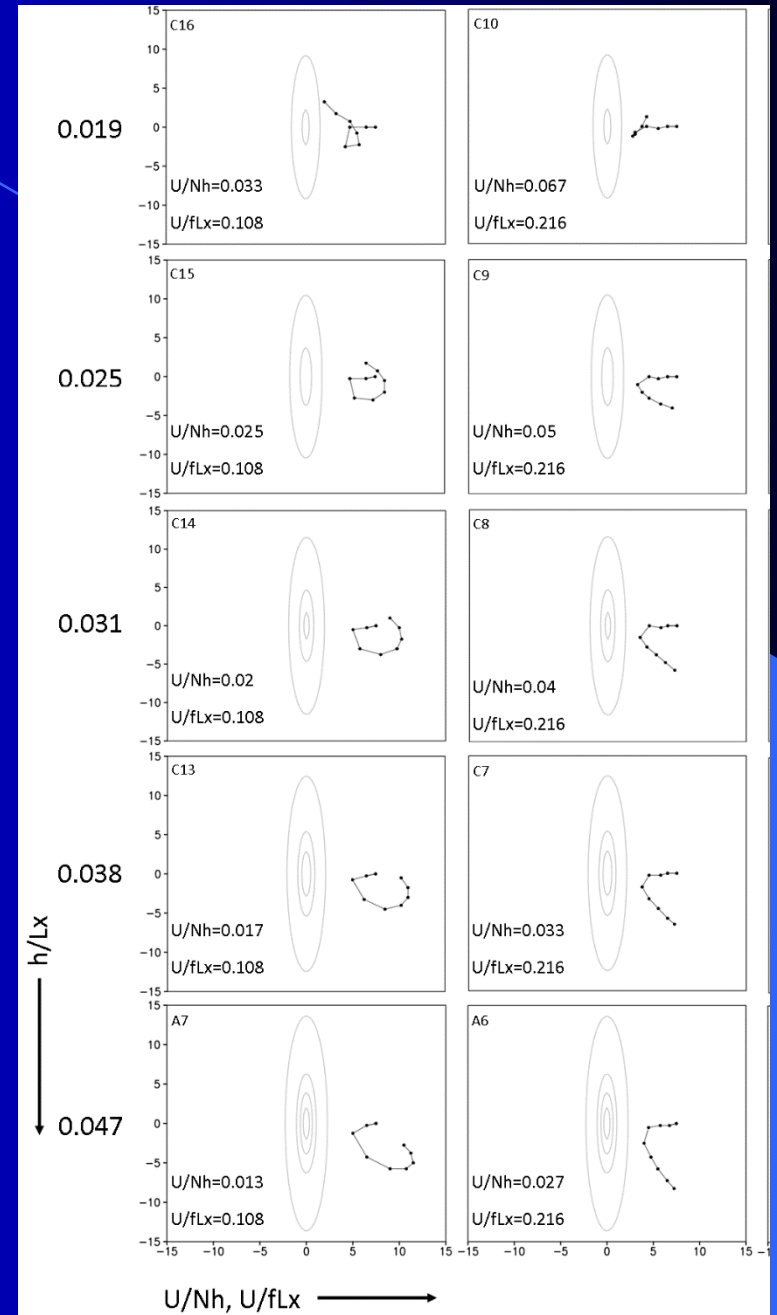


(a) V wind and radar echoes (contours) on E-W vertical xsec across the TC center at 186 h. (b-d) total water content on 325, 850, and 500 mb at 186 h.

B.6 Looping Tracks

In a recent study (Huang and Lin 2017 MAAP), it is found that looping tracks tend to occur under

- (i) small U/Nh and U/fL_x
(slow movement => subgeostrophic flow)
- (ii) large V_{max}/Nh
(strong TC rotation)
- (iii) moderate h/L_x ,
(moderate steepness)



B.7 Conclusions (Part B)

- TC movement can be predicted by the maximum vorticity tendency (∇T).
- Upstream of the mountain, orographic blocking makes the flow subgeostrophic which advects the TC to the south, like advecting of a point vortex.
- TC passes over the mountain anticyclonically, mainly steered by the mountain-generated high pressure.
- Over the lee slope and downstream of the mountain, the northwestward movement is enhanced by asymmetric diabatic heating, making the turning more abrupt.
- Far downstream of the mountain, the ∇T is mainly contributed by the horizontal vorticity advection of the basic wind.

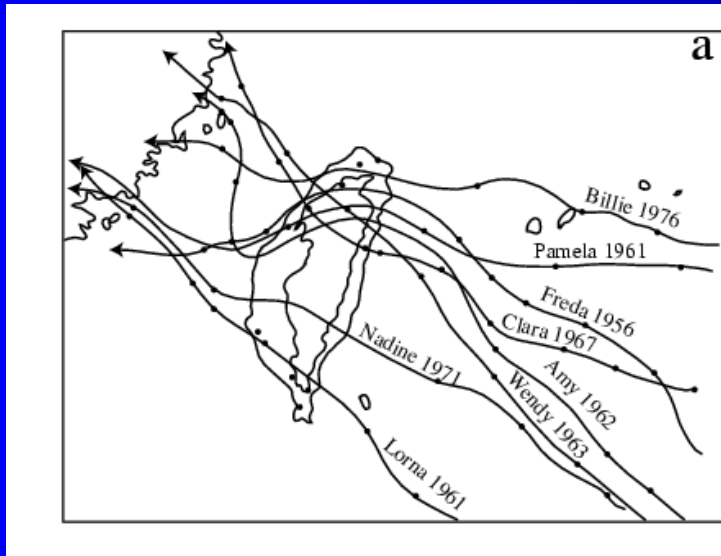
Thanks!

Part B: Orographic Influence on TC Tracks

B.1 Introduction

- QPF of orographic TC rain requires a good prediction of typhoon track, which needs a better understanding.
- **One well-known problem is the continuity of typhoon tracks over Taiwan's Central Mountain Range (CMR)** (Wang 1980; see Lin et al. 1999JAS or Lin 2007 for brief review).

Continuous Track



Discontinuous Track

